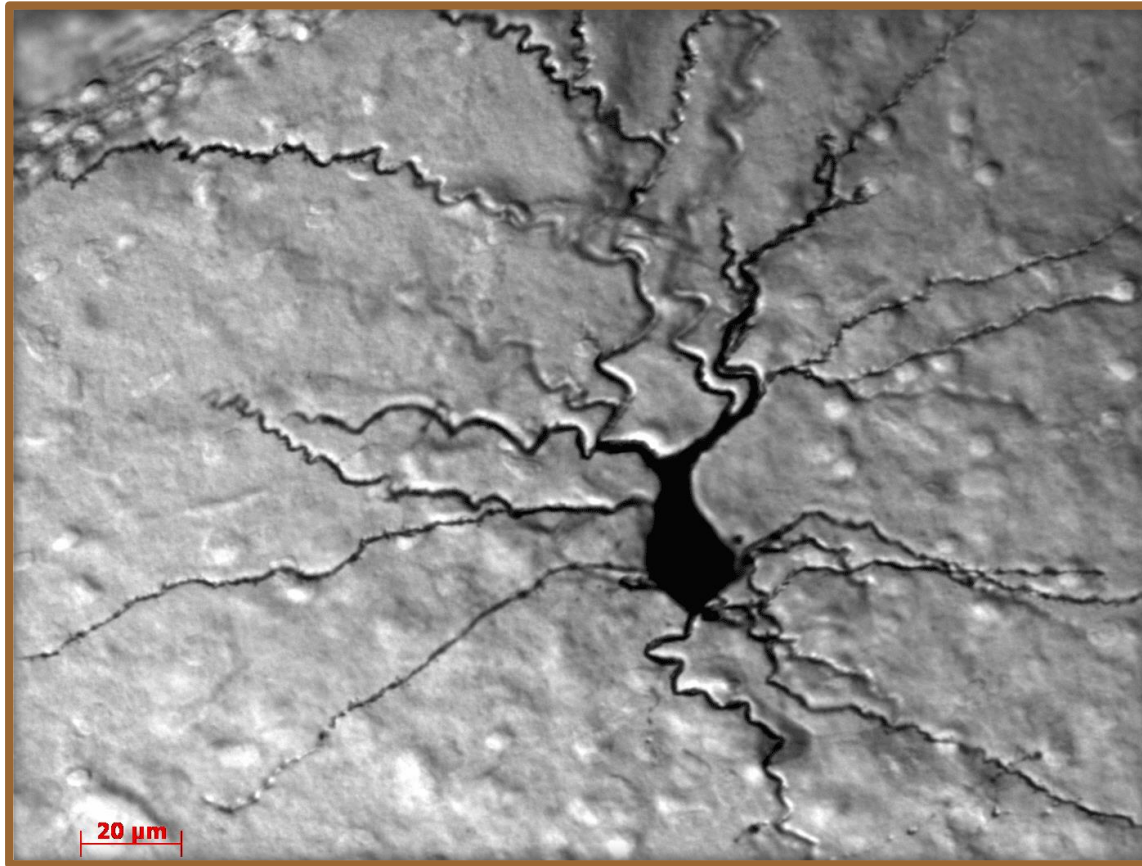


The neuron



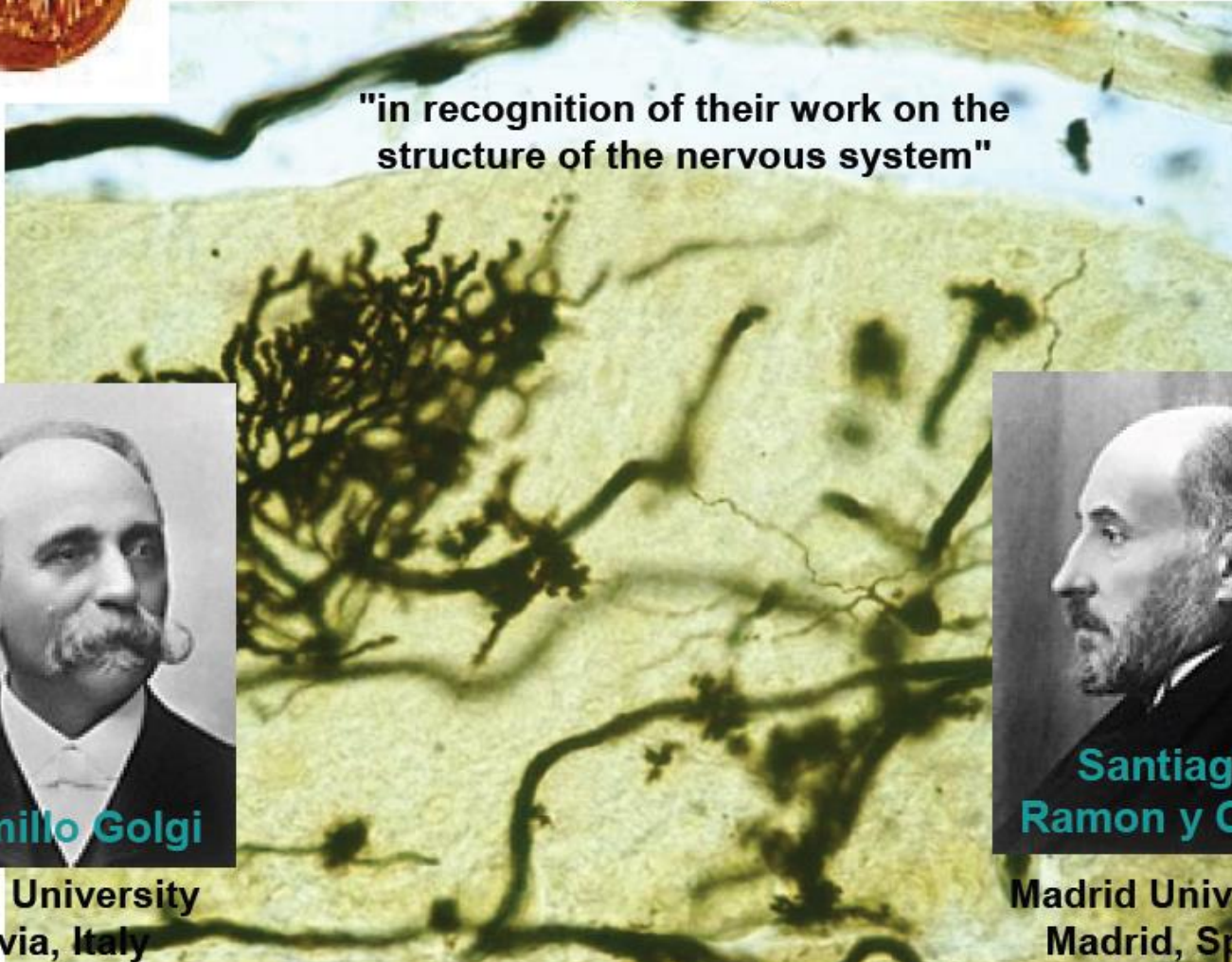
Biocytin labeled pyramidal neuron recorded in piriform cortex

Discovery of the neuron



The Nobel Prize in Physiology or Medicine 1906

"in recognition of their work on the structure of the nervous system"



Camillo Golgi

Pavia University
Pavia, Italy



**Santiago
Ramon y Cajal**

Madrid University
Madrid, Spain

The nervous system as a diffuse reticular syncytium?

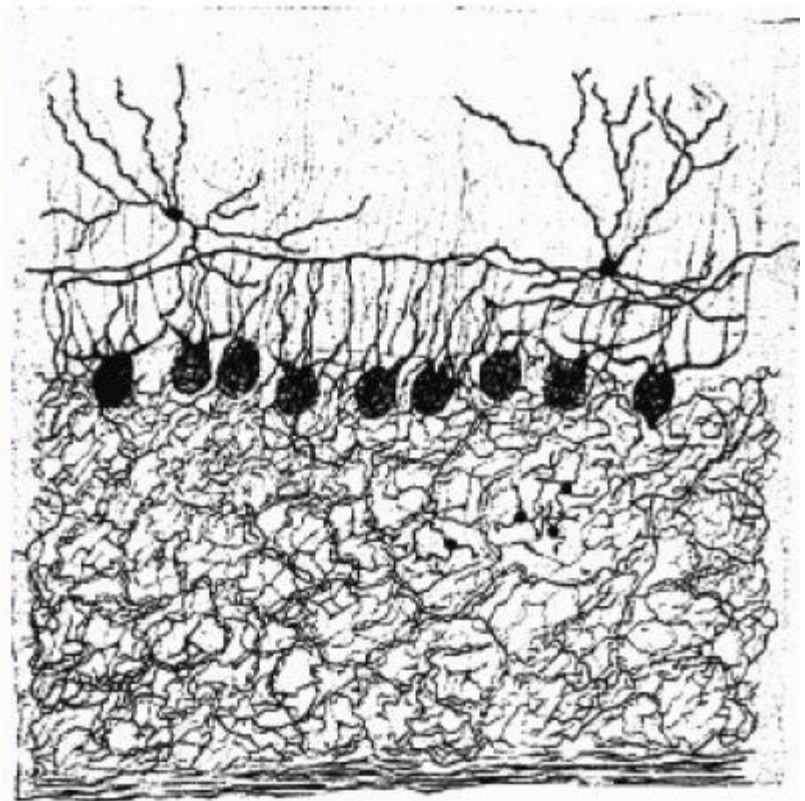
(i.e. a mass of cytoplasm with many nuclei but no internal cell boundaries)

Camillo Golgi

Nobel Lecture December 11, 1906

The Neuron Doctrine- theory and facts.

“..Far from being able to accept the idea of the individuality and independence of each nerve element, I have never had reason, up to now, to give up the concept which I have always stressed, that nerve cells, instead of working individually, act together, so that we must think that several groups of elements exercise a cumulative effect on the peripheral organs through whole bundles of fibers.”

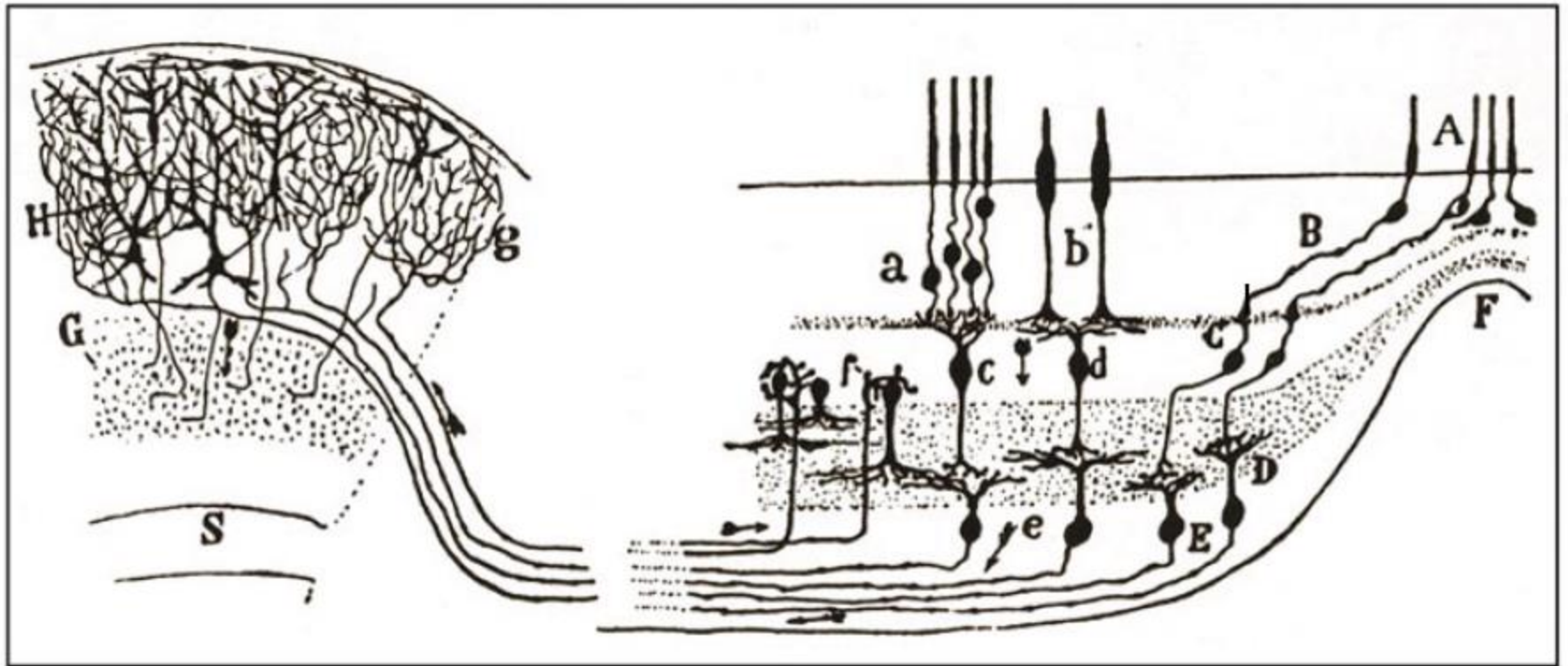


The Neuron Doctrine: (Santiago Ramon y Cajal)

Neurons are cells.

Each is an individual entity anatomically, embryologically, and functionally.

Also: Neurons have a functional polarity.



(A) Reticularist Doctrine

(B) Neuron Doctrine

Exception.....

....GAP JUNCTIONS
between neurons

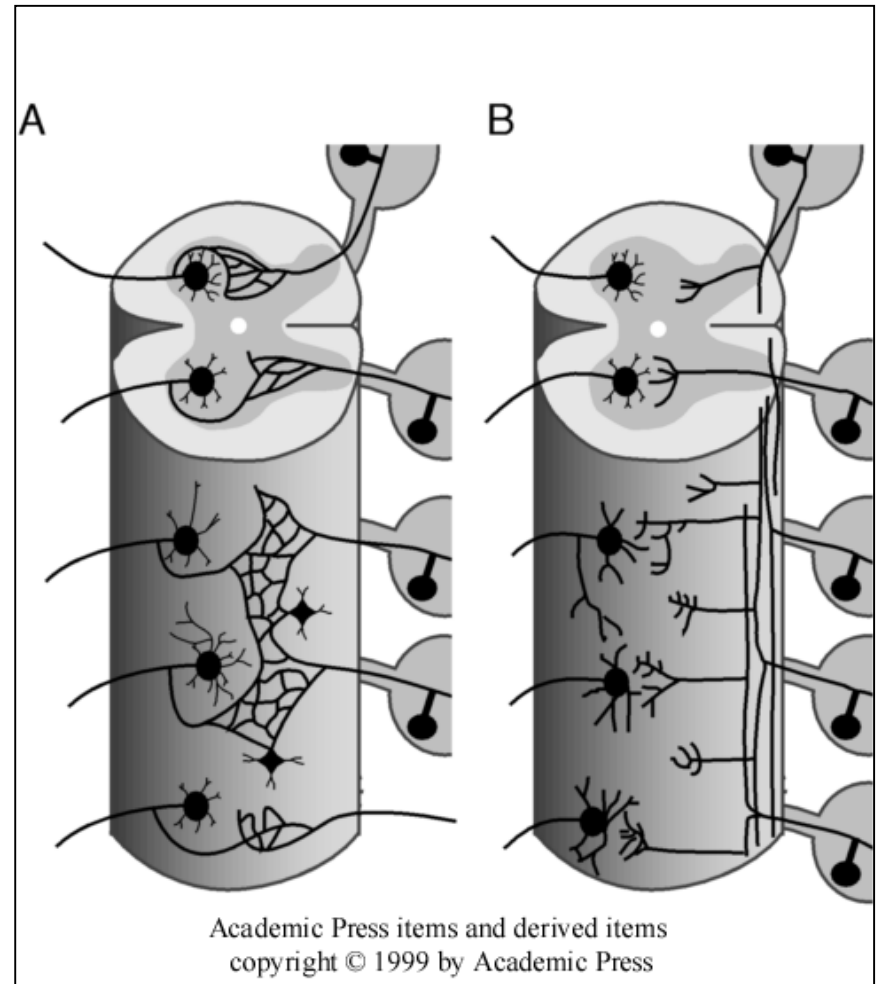
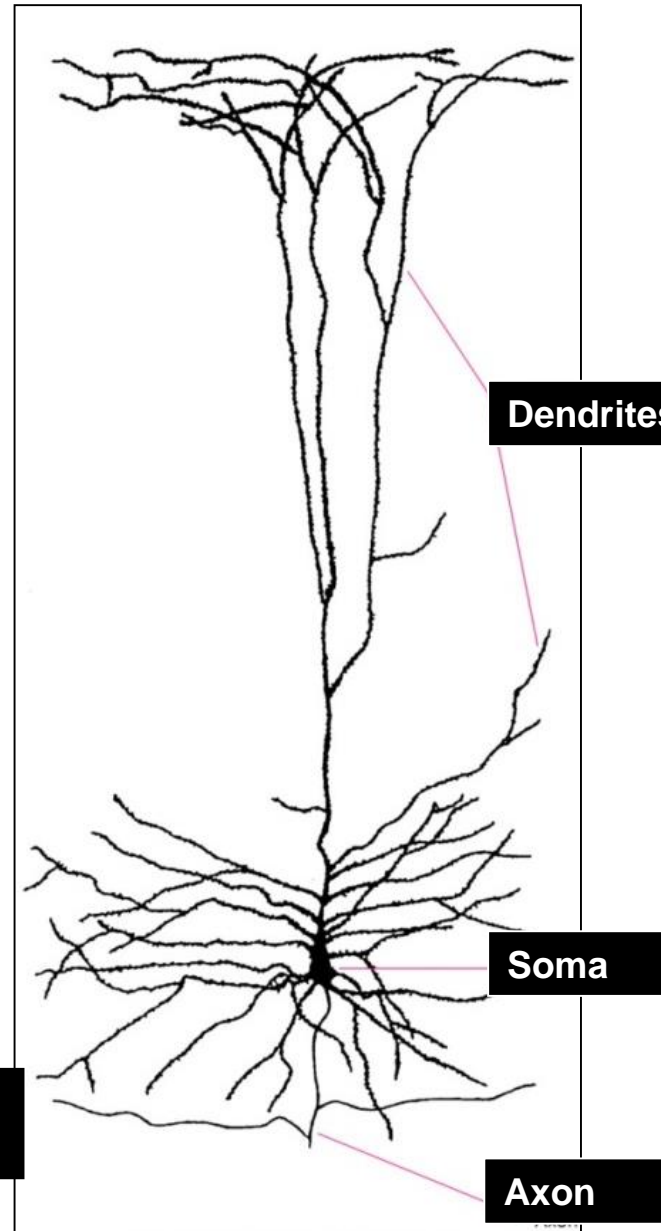


FIGURE 2 The nervous system is a reticulum versus the neuron doctrine. (A) Proponents of the reticularist's view of the nervous system believed that neurons are physically connected to one another, forming an uninterrupted network. (B) The neuron doctrine, in contrast, considers each neuron an individual entity that communicates with target cells across an appropriate intercellular gap. Adapted from Cajal (1911–1913).

Neuronal shape

Pyramidal neuron
(multipolar)



Dendrites

Soma

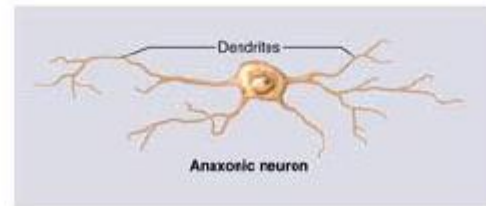
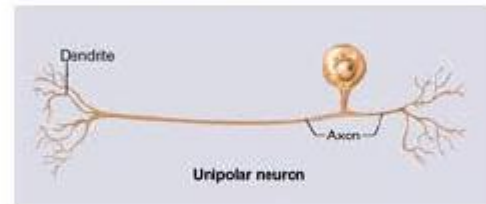
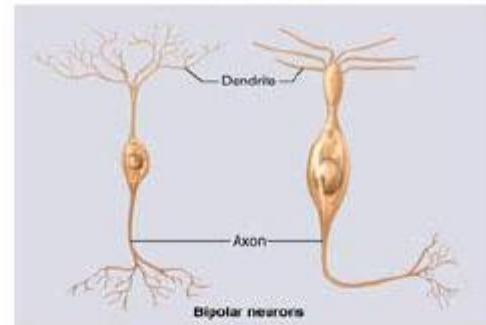
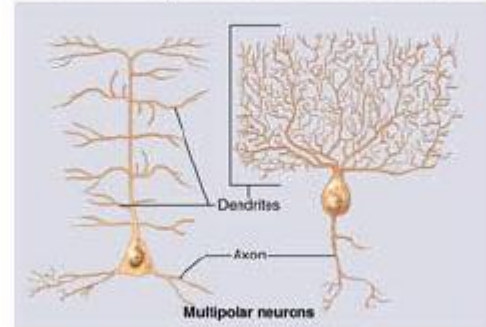
Axon

Variation in Neural Structure

Copyright © The McGraw-Hill Companies, Inc. Permission required for reproduction or display.

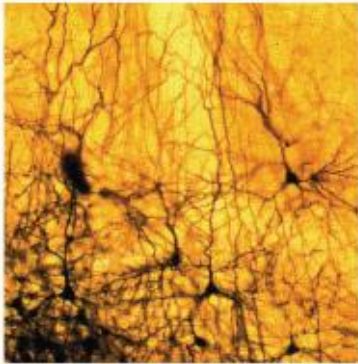
Basic classification of neurons

- **Multipolar neuron**
 - most common
 - many dendrites/one axon
- **Bipolar neuron**
 - one dendrite/one axon
 - olfactory, retina, ear
- **Unipolar neuron (pseudounipolar)**
 - sensory from skin and organs to spinal cord
- **Anaxonic neuron**
 - many dendrites/no axon
 - help in visual processes



Studying structure

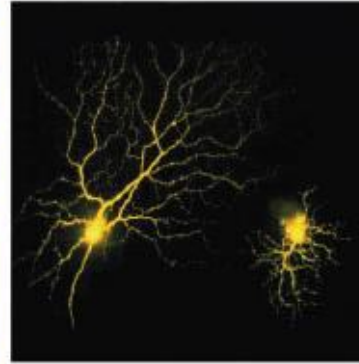
(A) Golgi stain/
cortical neurons



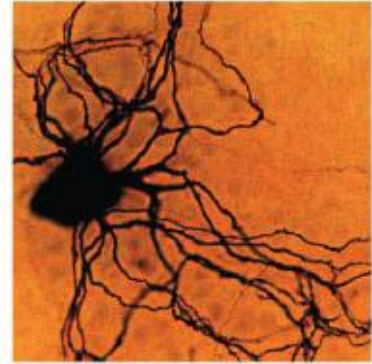
(B) Golgi stain/
Purkinje neurons



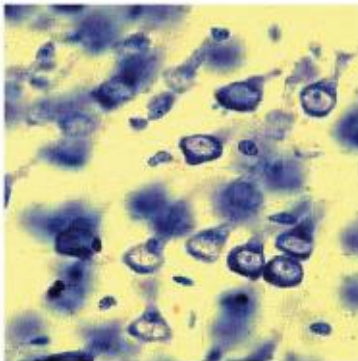
(C) Dye injection/
retinal neurons



(D) HRP (enzyme) injection/
autonomic neuron

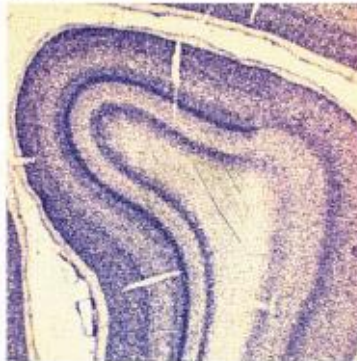


(E)



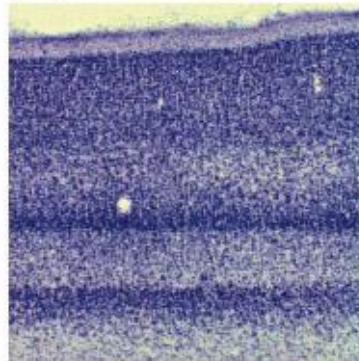
Cresyl violet/RNA/
cortical neurons

(F)

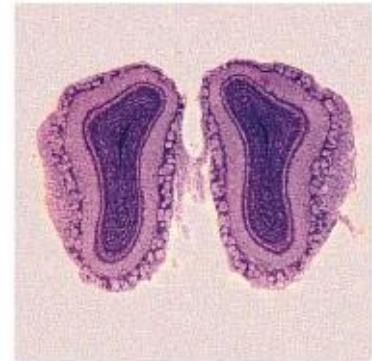


Nissl stain/RNA/
cortical neurons

(G)



(H)



Nissl stain/
olfactory bulb

NEUROSCIENCE, Fourth Edition, Figure 1.6

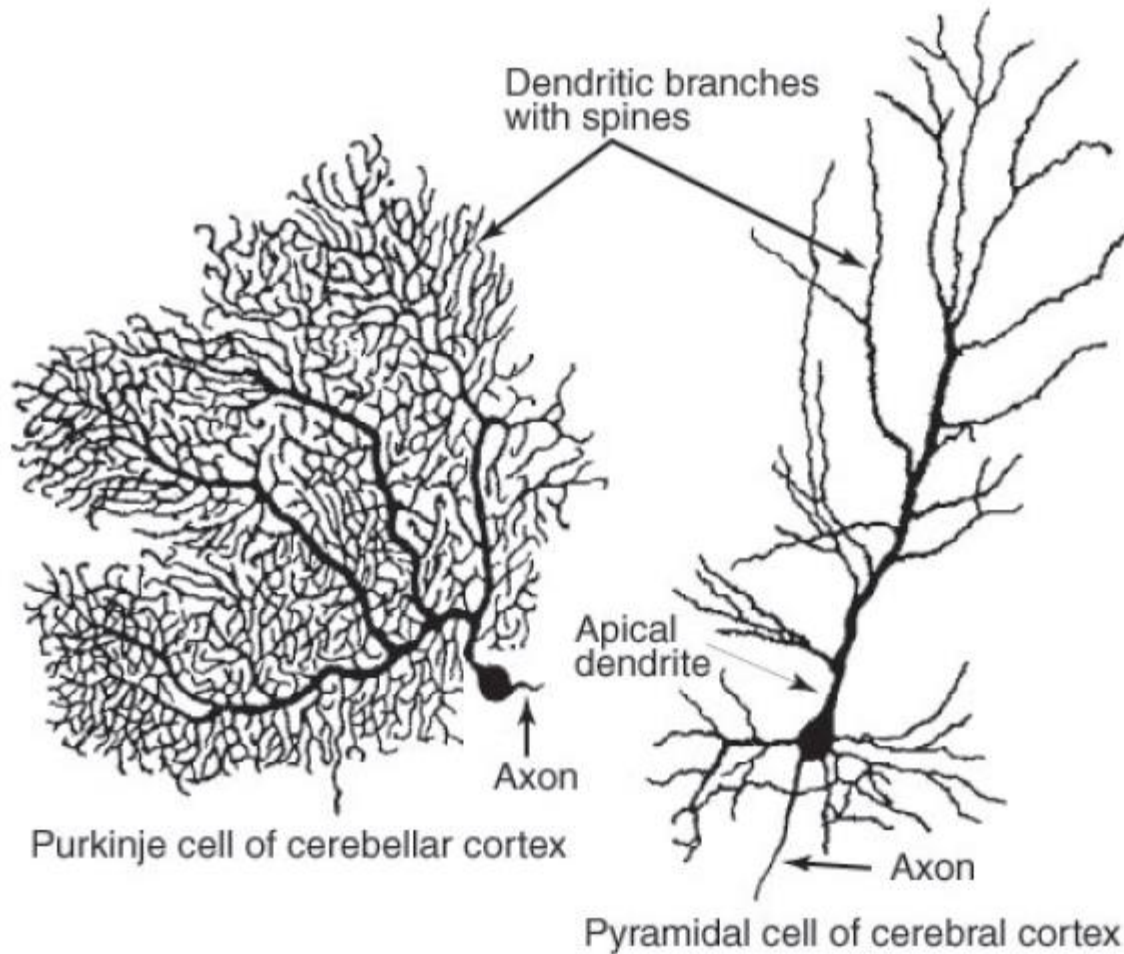
© 2008 Sinauer Associates, Inc.



<https://www.jove.com/science-education/5204/an-introduction-to-neuroanatomy>

<https://www.jove.com/science-education/5206/histological-staining-of-neural-tissue>

Morphology of vertebrate multipolar neurons is highly variable



Differences in arbor density reflect differences in connectivity

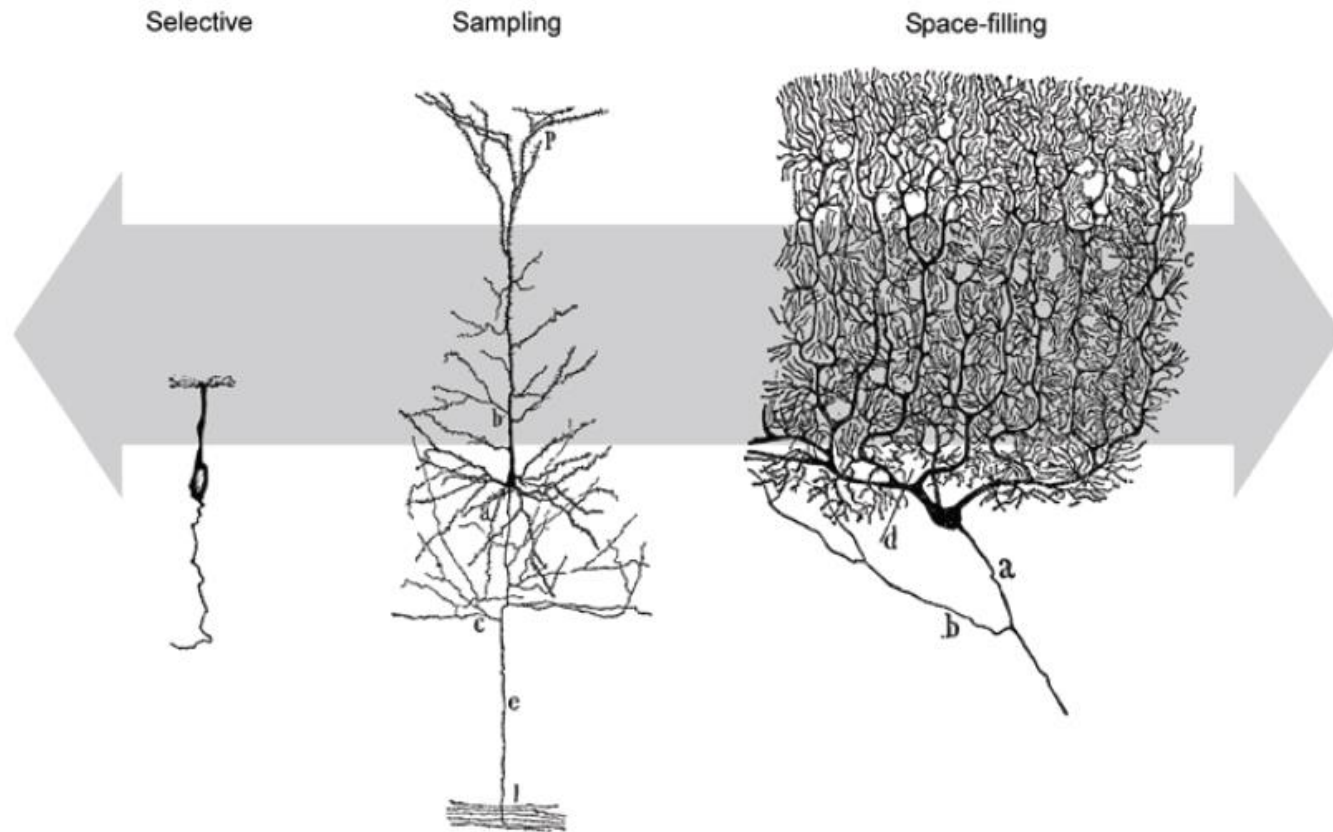


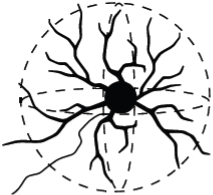
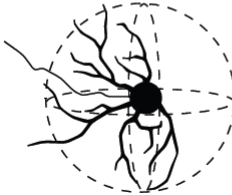

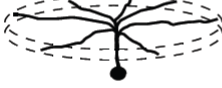


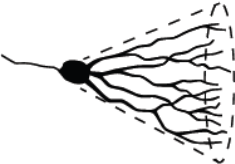
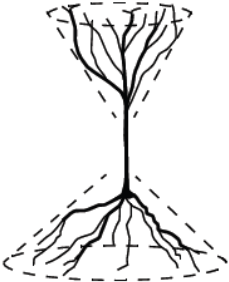



Fig. 1.5 The densities of dendritic arbors lie on a continuum of values. Differences in arbor density reflect differences in connectivity. At one extreme are selective arborizations in which each dendrite connects the cell body to a single remote target. An olfactory sensory cell is used to illustrate this. At the other extreme lie space-filling arborizations in which the dendrites cover a region, as with the cerebellar Purkinje cell. Intermediate arbor densities are referred to as sampling arborizations, as demonstrated by a pyramidal cell from cerebral cortex. (Drawings of neurons from Ramón y Cajal, 1995.)

Characteristic arborization patterns

Pattern	Characteristics	Examples
Adendritic 	Cell body lacks dendrites	Dorsal root ganglion cells Sympathetic ganglion cells
Spindle radiation 	Two dendrites emerge from opposite poles of the cell body and have few branches	Lugaro cells Bipolar cells of cortex
Spherical radiation Stellate 	Dendrites radiate in all directions from cell body	Spinal neurons Neurons of subcortical nuclei (e.g. inferior olive, pons, thalamus, striatum) Cerebellar granule cells
Partial 	Dendrites radiate from cell body in directions restricted to a part of a sphere	Neurons at edges of "closed" nuclei (e.g. Clarke's column, inferior olive, vestibular nuclei)
Laminar radiation Planar 	Dendrites radiate from cell body in all directions within a thin domain	Retinal horizontal cells
Offset 	Plane of radial dendrites offset from cell body by one or more stems	Retinal ganglion cells
Multi 	Cell has multiple layers of radial dendrites	Retinal amacrine cells

Characteristic arborization patterns

Pattern	Characteristics	Examples
Cylindrical radiation 	Dendrites ramify from a central soma or dendrite in a thick cylindrical (disk-shaped) domain	Pallidal neurons Reticular neurons
Conical radiation 	Dendrites radiate from cell body or apical stem within a cone or paraboloid	Granule cells of dentate gyrus and olfactory bulb Primary dendrites of mitral cells of olfactory bulb Semilunar cells of piriform cortex
Biconical radiation 	Dendrites radiate in opposite directions from the cell body	Bitufted, double bouquet, and pyramidal cells of cerebral cortex Vertical cells of superior colliculus
Fan radiation 	One or a few dendrites radiate from cell body in a flat fan shape	Cerebellar Purkinje cells

What changes among the dendrites ?

Table 1.1 Typical dimensions of dendrites for a few types of neurons

Neuron	Average soma diameter (μm)	Number of dendrites at soma	Proximal dendrite diameter (μm)	Number of branch points	Distal dendrite diameter (μm)	Dendrite extent* (μm)	Total dendritic length (μm)
Cerebellar granule cell (cat)	7	4	1	0	0.2–2	15	60
Starburst amacrine cell (rhesus)	9	1	1	40	0.2–2	120	—
Dentate gyrus granule cell (rat)	14	2	3	14	0.5–1	300	3200
CA1 pyramidal cell (rat)	21						11900
basal dendrites		5	1	30	0.5–1	130	5500
stratum radiatum		1	3	30	0.25–1	110	4100
stratum lacunosum-moleculare				15	0.25–1	500	2300
Cerebellar Purkinje cell (guinea pig)	25	1	3	440	0.8–2.2	200	9100
Principal cell of globus pallidus (human)	33	4	4	12	0.3–0.5	1000	7600
Meynert cell of visual cortex (macaque)	35						15400
basal dendrites		5	3	—	—	250	10200
apical dendrites		1	4	15	2–3	1800	5200
Spinal α -motoneuron (cat)	58	11	8	120	0.5–1.5	1100	52000

*The average distance from the cell body to the tips of the longest dendrites.

Sources: Ito (1984); Mariani (1990); Claiborne et al. (1990); Bannister and Larkman (1995a); Rapp et al. (1994); Palay (1978); Yelnik et al. (1984); Ulfhake and Kellerth (1981).

Methods for measuring dendritic complexity

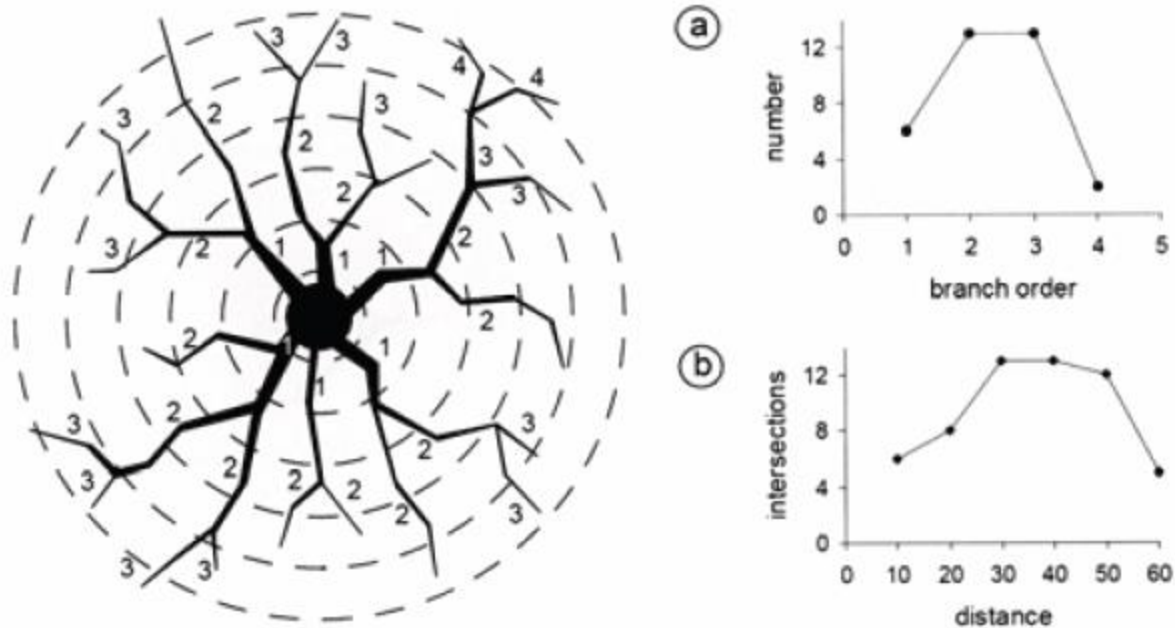
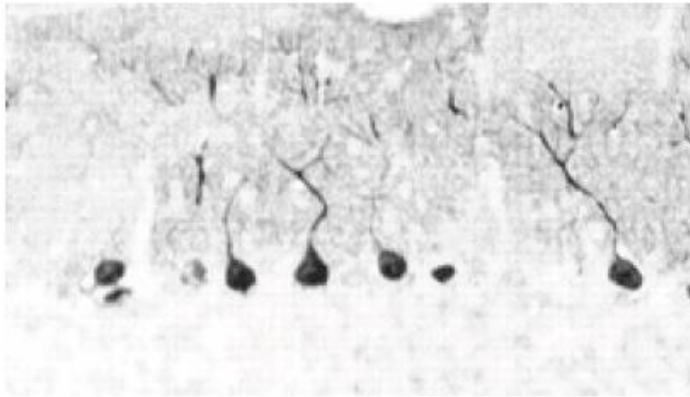


Fig. 1.4 Methods for characterizing dendritic branching. (a) A plot of the number of branches of each order using the centrifugal method of branch ordering. The *Strahler method* is similar but the dendritic tips are order 1 and branch numbers increase sequentially toward the soma. (b) A *Sholl plot* showing the number of intersections of the dendritic tree with circles of increasing radius from the center of the dendritic arbor. When three-dimensional data are available, concentric spheres are used rather than these circles centered on a two-dimensional projection of the neuron.

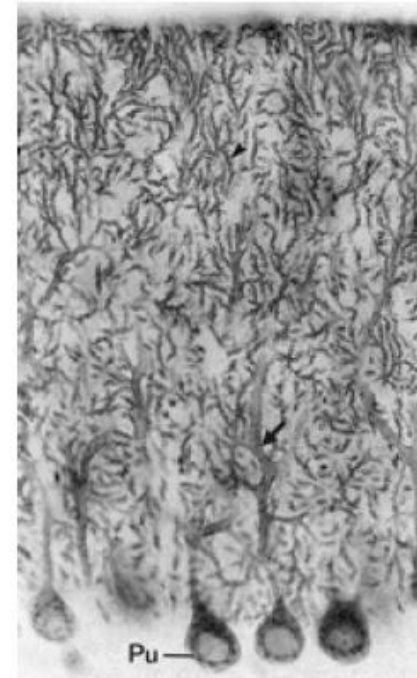
Functional classification of neurons

- **Sensory (afferent) neurons**
 - detect changes in body and external environment
 - information transmitted into brain or spinal cord
- **Interneurons (association neurons)** • **Projection neurons**
 - **Local circuit neurons**
 - lie between sensory and motor pathways in CNS
 - 90% of our neurons are interneurons
 - process, store and retrieve information
- **Motor (efferent) neuron**
 - send signals out to muscles and gland cells
 - organs that carry out responses called effectors

Neurons can also be identified by immunocytochemistry

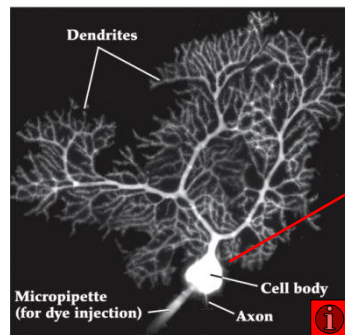
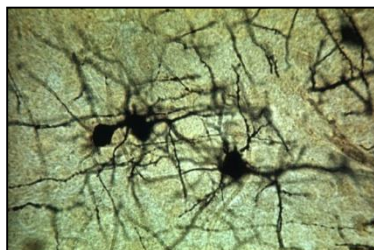
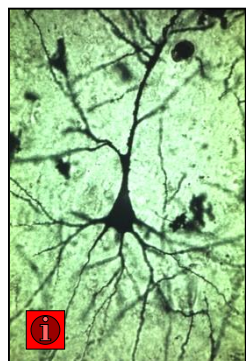
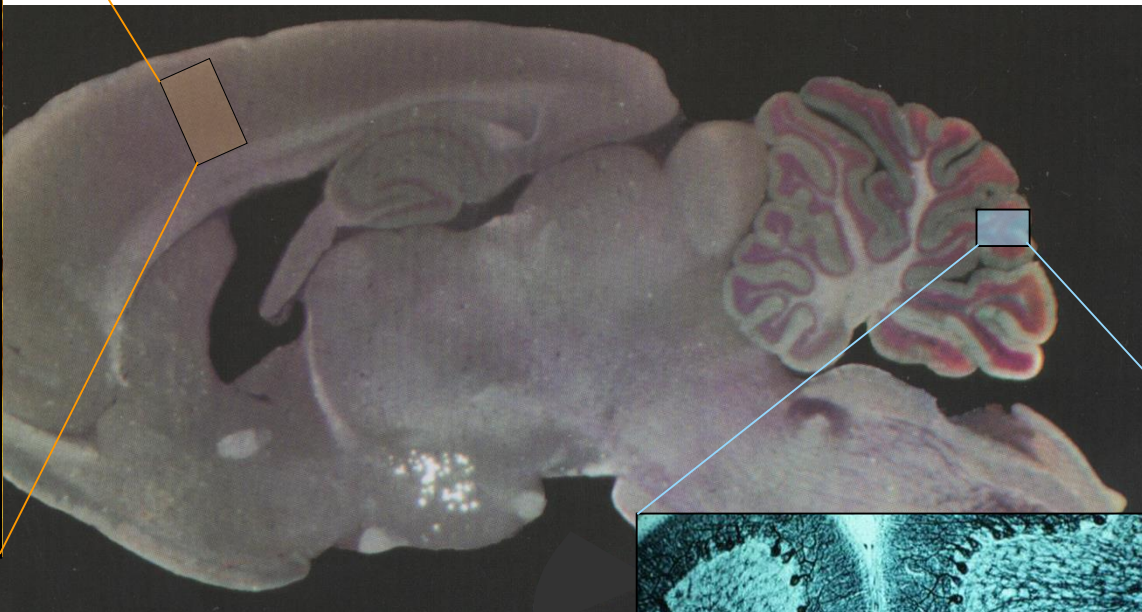
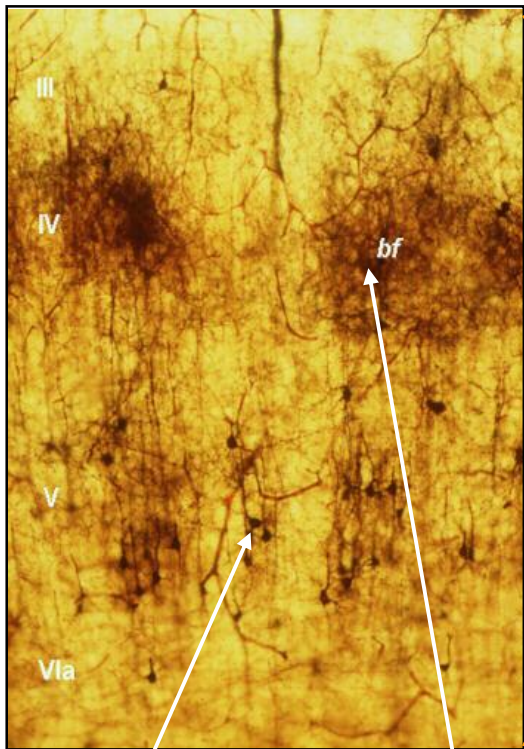


calbindin

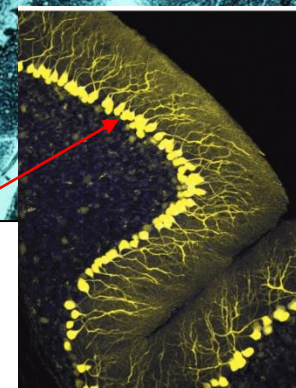
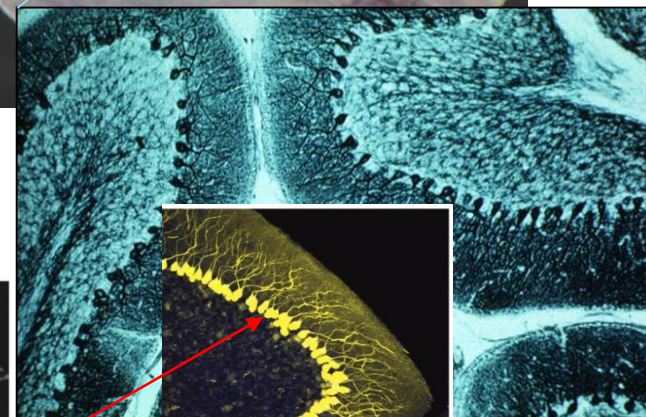


Glutamate transporter
EAAT4

Various NEURONAL TYPES in the mammalian brain

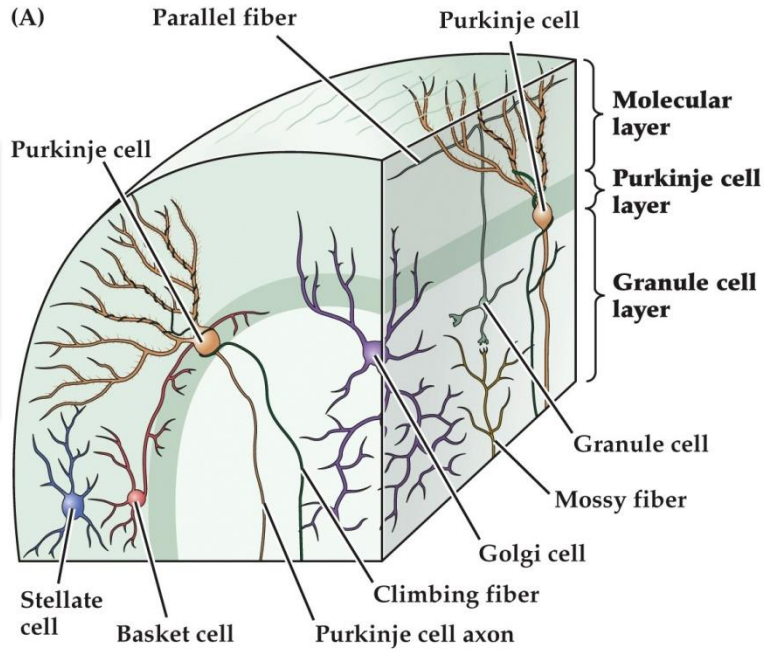


SCIENCE 5e, Figure 19.8 (Part 1)
Pearson Associates, Inc.

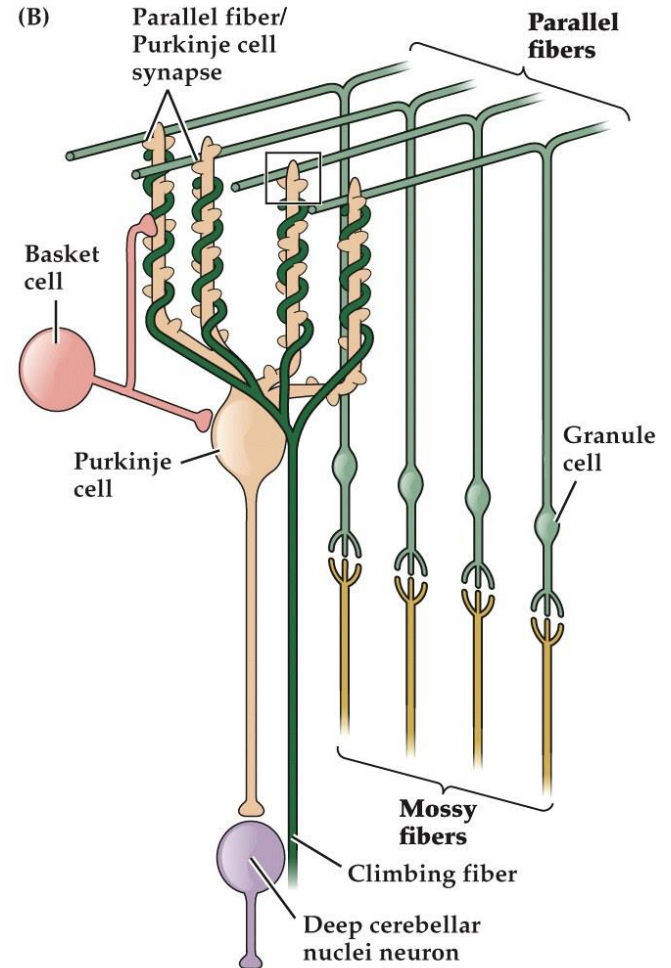
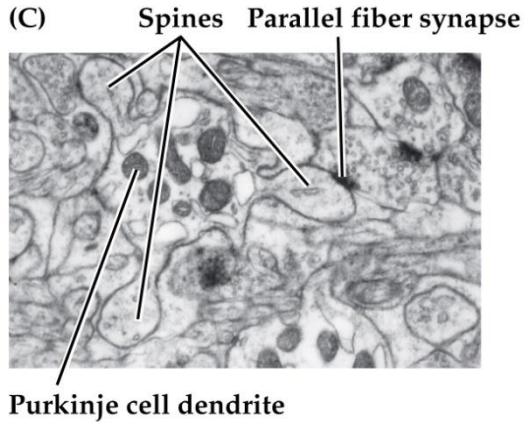


SCIENCE 5e, Figure 19.8 (Part 2)
Pearson Associates, Inc.

Morphology and neuronal types in the cerebellum



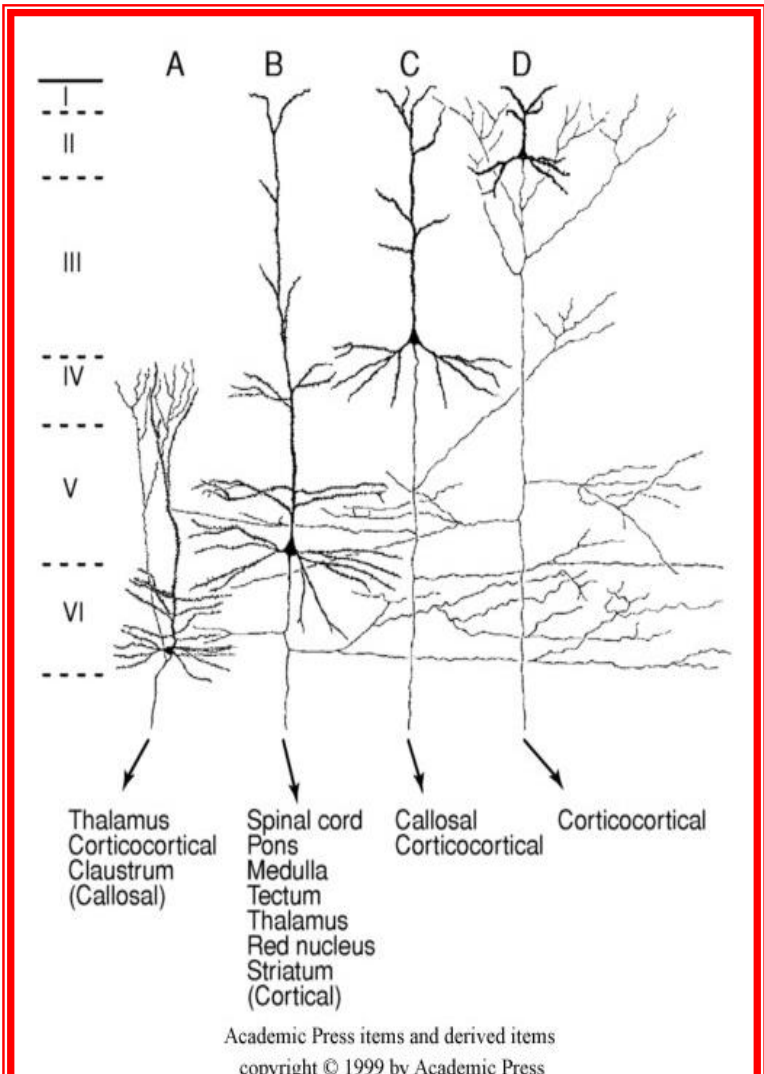
NEUROSCIENCE 5e, Figure 19.9 (Part 1)
© 2012 Sinauer Associates, Inc.



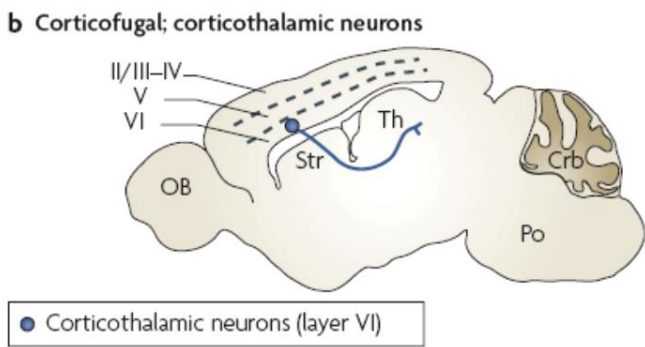
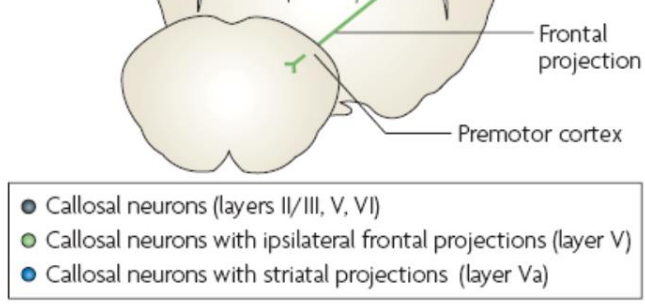
NEUROSCIENCE 5e, Figure 19.9 (Part 2)
© 2012 Sinauer Associates, Inc.

Molecular/functional heterogeneity of Purkinje cells?

Morphology and distribution of pyramidal neurons in the neocortex



a Commissural; callosal projection neurons → These pyramidal n. never project axons to targets outside the telencephalon



Molyneaux et al., 2007

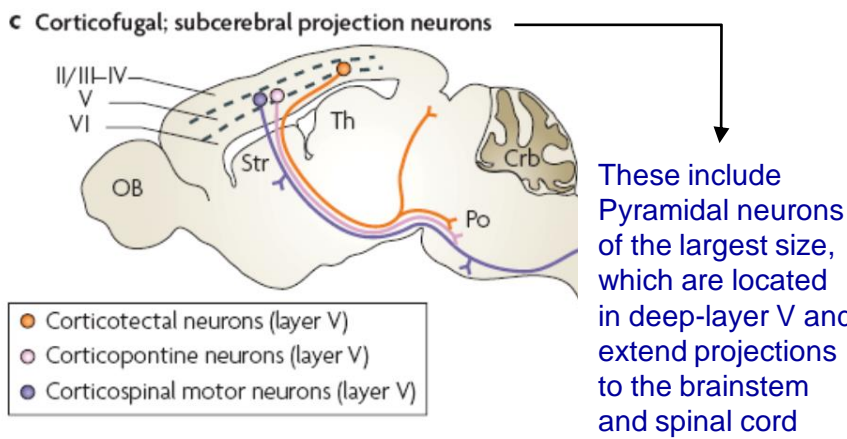


FIGURE 4 Morphology and distribution of neocortical pyramidal neurons. Note the variability in cell size and dendritic arborization, as well as the presence of axon collaterals, depending on the laminar localization (I–VI) of the neuron. Also, different types of pyramidal neurons with a precise laminar distribution project to different regions of the brain. Adapted from Jones (1984).

Neocortical interneurons diversity

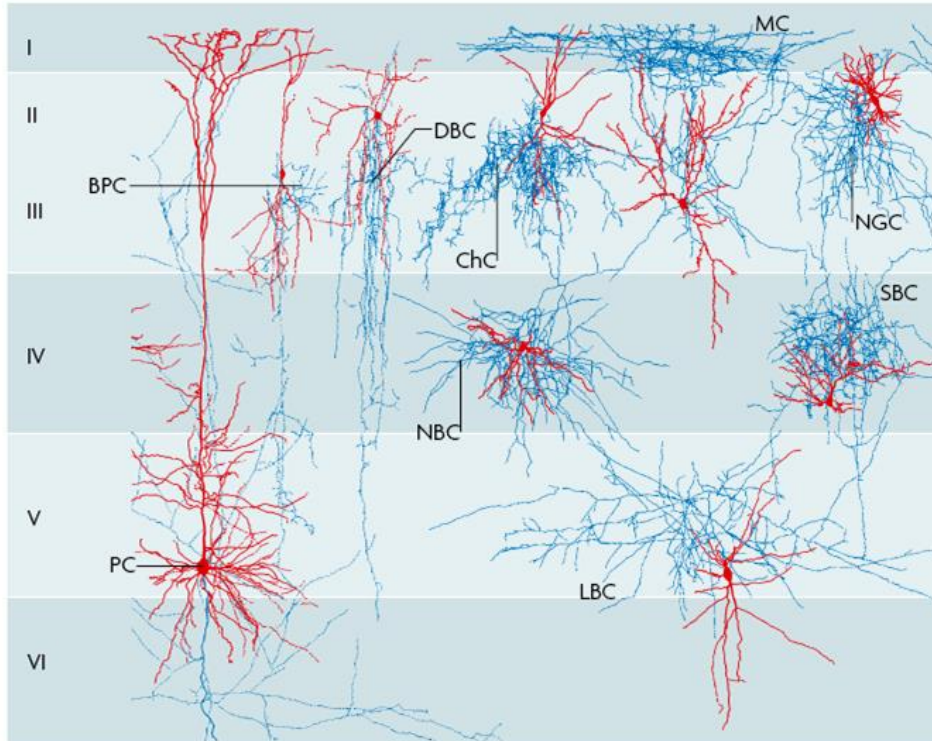


Figure 1 | Axon arbors and innervation patterns of neocortical interneurons. Interneuron axon arbors distribute inhibitory outputs to discrete spatial domains in the neural network. The figure shows a reconstruction of several classes of neocortical interneurons and, for comparison, a layer five pyramidal neuron (PC; left most). Axons are shown in blue and dendrites are shown in red. The geometry of interneuron axon arbors can be vertical, horizontal, or laminated, suggesting that their output can be distributed to the same or multiple cortical columns, and same or multiple cortical layers. Interneuron axons often elaborate highly exuberant local branches, innervate specific cell types, and impose strong control over local neural populations. Cortical layers are indicated on the left of the figure. BPC, bipolar cell; ChC, chandelier cell; DBC, double bouquet cell; LBC, large basket cell; MC, Martinotti cell; NBC, nested basket cell; NGC, neurogliaform cell; SBC, small basket cell. Images courtesy of Dr Henry Markram (EPFL, Switzerland).

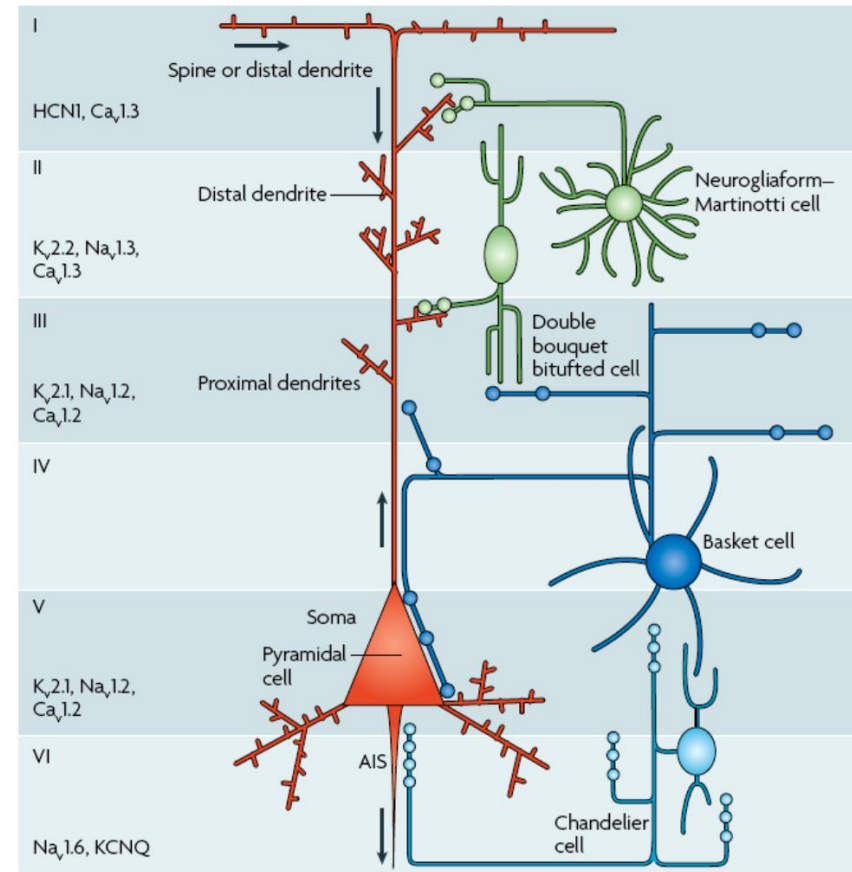


Figure 2 | The subcellular organization of GABAergic inputs. Pyramidal neurons (shown in red) in the neocortex are characterized by their large size, striking polarity and distinct subcellular domains. The compartmentalized forward and backward electrical signalling (depicted by arrows) arises from the targeted distribution of signalling mechanisms, receptors and ion channels. The distributions of several voltage-gated sodium (Na_v), potassium (K_v ; KCNQ) and calcium (Ca_v) channels, and of a hyperpolarization-activated cyclic nucleotide-gated (HCN) cation channel are highlighted to the left of the pyramidal neuron. The subcellular organization of different classes of GABAergic inhibitory inputs is superimposed on the anatomical and physiological compartments of pyramidal neurons, allowing effective regulation of synaptic integration, spike generation, back propagation and plasticity. The stereotyped position and geometry of pyramidal neurons within a cortical column (cortical layers are indicated on the left) suggests that their subcellular architecture significantly affects neuronal signalling in cortical circuits. AIS, axon initial segment; GABA, γ -aminobutyric acid. Modified, with permission, from *Nature Rev. Neurosci.* REF. 27 © (2005) Macmillan Publishers Ltd.

“Easy” neuronal classification

Structural classification:

Unipolar, bipolar, multipolar, more ...

Functional classification:

- projection (inter)neurons
- local circuit (inter)neurons

- excitatory (neurotransmitters: Glutamate, etc.)
- inhibitory (neurotransm.: GABA, glycine, etc.)

The problem of neuronal classification and subtype identification.....

We need to classify different neuronal types in order to speak a “common language” with other neuroscientists and in order to understand the complexity of brain function...

HOW should we classify neurons?

By morphology?

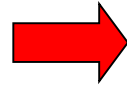
By functional features?

By expression markers?

How do we put together information from different approaches?

for discussion see [Yuste, 2005](#)

The problem of neuronal classification...



The obvious (but not the easiest) solution would be COMBINING different approaches in the same experimental model. An example:

Localization of Calcium-binding Proteins in Physiologically and Morphologically Characterized Interneurons of Monkey Dorsolateral Prefrontal Cortex

A.V. Zaitsev¹, G. Gonzalez-Burgos¹, N.V. Povysheva¹, S. Kröner^{2,3}, D.A. Lewis^{1,2} and L.S. Krimer¹

Cerebral Cortex August 2005;15:1178-1186

ABSTRACT

In the primate neocortex, little is known about the possible associations between functional subclasses of GABA neurons, their morphological properties and calcium-binding protein (CaBP) content. We used whole-cell current clamp recordings, combined with intracellular labeling and fluorescence immunohistochemistry, to determine these relationships for interneurons in layers 2-3 of monkey prefrontal cortex (PFC). Eighty-one interneurons were included in the analysis. Thirty-eight of these cells showed immunoreactivity for one of the three CaBPs tested. Co-localization of more than one CaBP was not observed in any of the interneurons examined. Interneurons with different CaBPs formed distinct populations with specific physiological membrane properties and morphological features. Parvalbumin (PV)-positive cells had the physiological properties characteristic of fast-spiking interneurons (FS) and the morphology of basket or chandelier neurons. Most calretinin (CR)-containing cells had the physiological properties ascribed to non-fast-spiking cells (non-FS) and a vertically oriented axonal morphology, similar to that of double bouquet cells. Calbindin (CB)-positive interneurons also had non-FS properties and included cells with double bouquet morphology or with a characteristic dense web of axonal collaterals in layer 1. Classification of the interneurons based on cluster analysis of multiple electrophysiological properties suggested the existence of at least two distinct groups of interneurons. The first group contained mainly PV-positive FS cells and the second group consisted predominantly of CR- and CB-positive non-FS interneurons. These findings may help to illuminate the functional roles of different groups of interneurons in primate PFC circuitry.

- (1) Whole-cell electrophysiological recording on cortical slices
- +
- (2) intracellular injection of biocytin in recorded neurons (for later recognition and morphological analysis)
- +
- (3) fluorescence immunocytochemistry for selected markers (calcium-binding proteins: parvalbumin, calbindin and calretinin)

The phenotype of **BC-injected/electrophysiologically-recorded** interneurons is determined by **immunocytochemistry**

Zaitsev et al., 2005

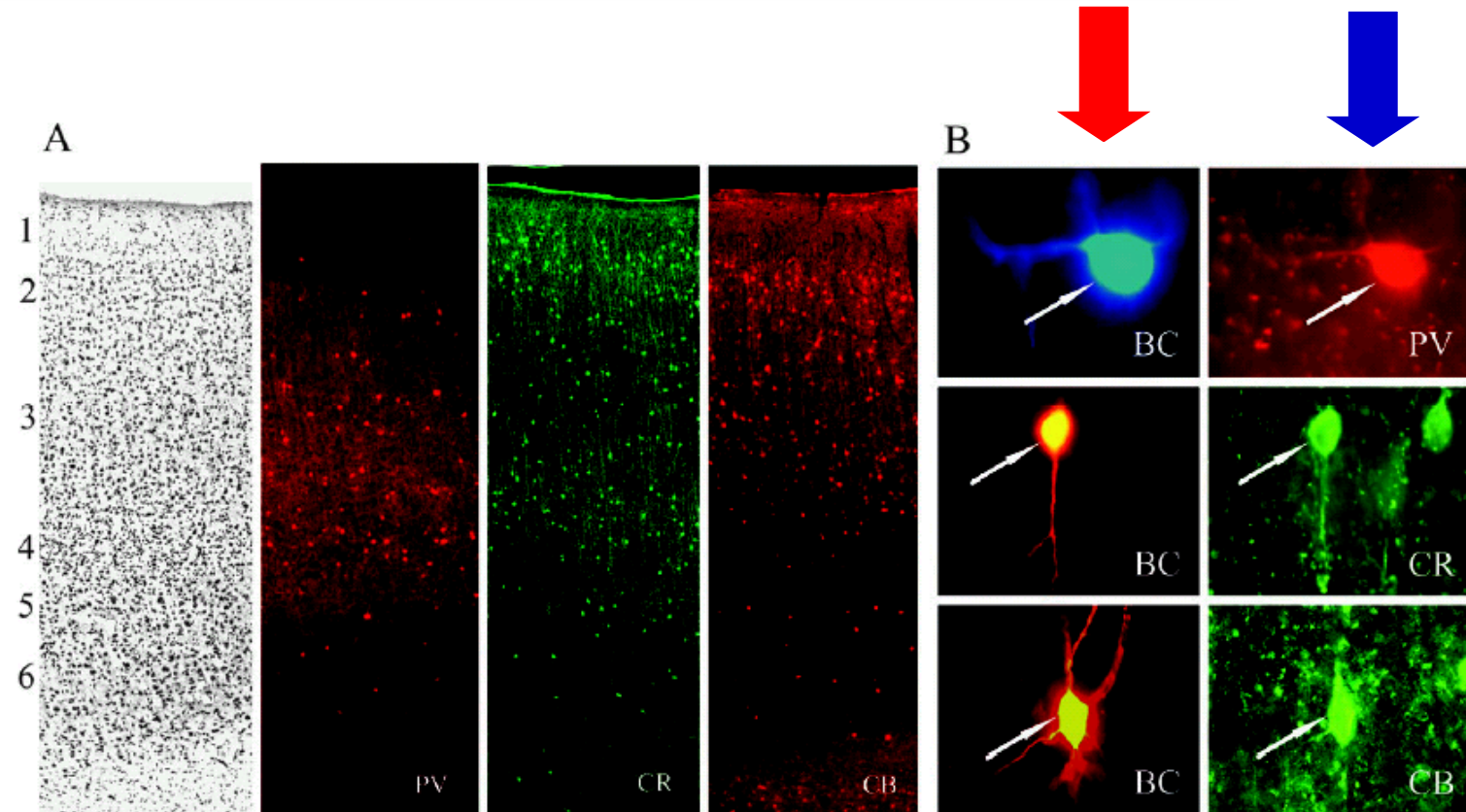


Figure 1. Fluorescence-labeling of CaBPs in monkey DLPFC interneurons. (A) Photomicrographs of adjacent coronal sections (area 46) with laminar boundaries; from left Nissl stain, PV-, CR- and CB-IR structures. Note the substantial differences in the laminar distribution of the neurons labeled for each CaBP. (B) Dual-label photomicrographs from the same microscopic field, showing immunohistochemical identification of physiologically characterized biocytin (BC)-injected interneurons as positive for PV, CR or CB. Arrows show the cell bodies. Top: BC visualized by streptavidin-Alexa Fluor[®] 350 conjugate (blue), PV-IR visualized by Alexa Fluor[®] 594 conjugated secondary antibody. Middle: BC visualized by streptavidin-Alexa Fluor[®] 568 conjugate, CR-IR visualized by Alexa Fluor[®] 488 conjugated secondary antibody. Bottom: BC visualized by streptavidin-Alexa Fluor[®] 568 conjugate, CB-IR visualized by Alexa Fluor[®] 488 conjugated secondary antibody.



<https://www.jove.com/science-education/5040/introduction-to-fluorescence-microscopy>

The combination of intracellular-injection techniques and immunocytochemistry suggests that the same phenotypic marker is expressed by interneurons with different morphologies

Do different morphologies indicate different functional features?

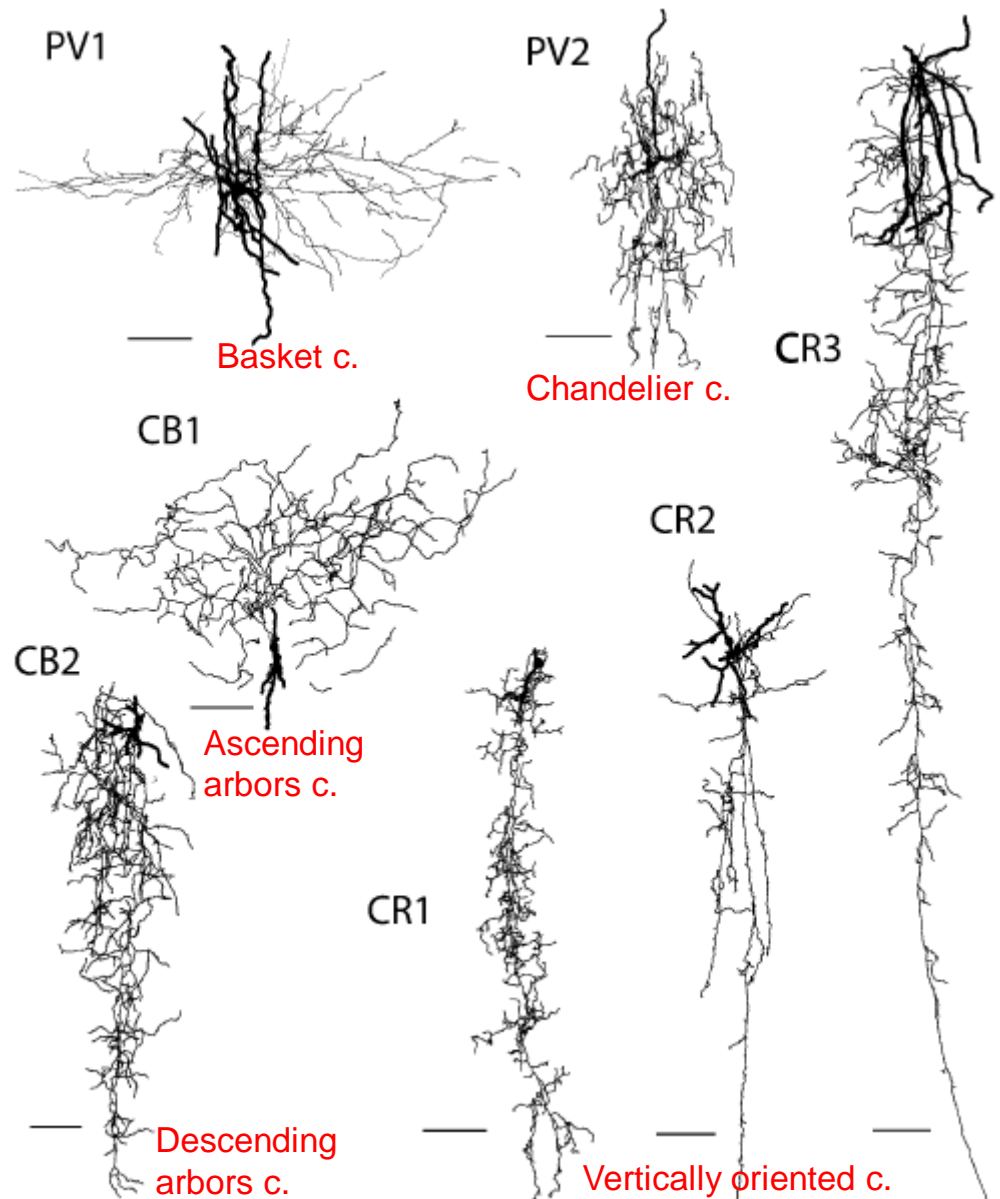


Figure 2. Three-dimensional reconstructions of biocytin-labeled interneurons from monkey DLPFC. PV1, PV-IR spreading arbor (basket) cell; PV2, PV-IR chandelier cell; CR1-CR3, examples of CR-IR vertically oriented cells; CB1, CB-IR cell with ascending arbors; CB2, CB-IR cell with descending arbors. Calibration bars = 100 μ m.

Data were processed using **CLUSTER ANALYSIS:** correlation between **electrophysiological properties** and **expression of specific Ca⁺-binding proteins**

When cells are grouped based only on electrophysiological properties, two main groups (= clusters) of interneurons are obtained: FS (Fast Spiking) and non-FS.

These two clusters do show significant differences in Ca⁺-binding protein content

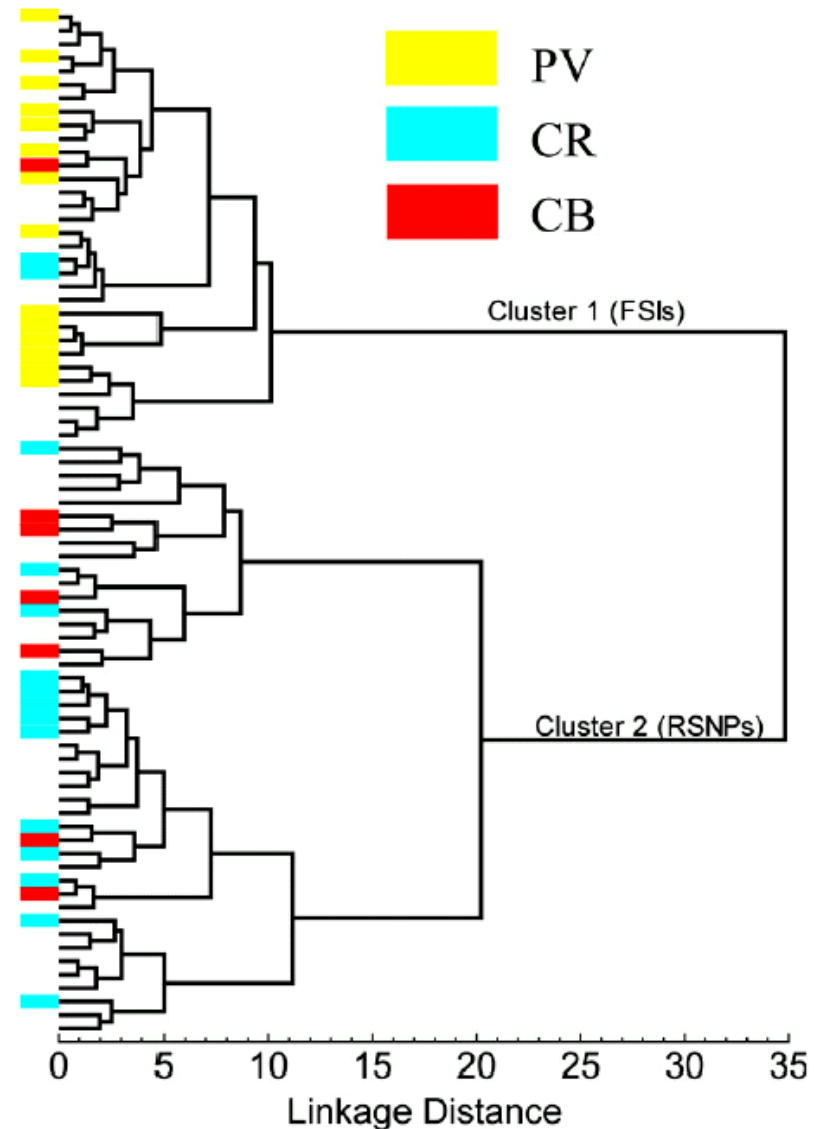
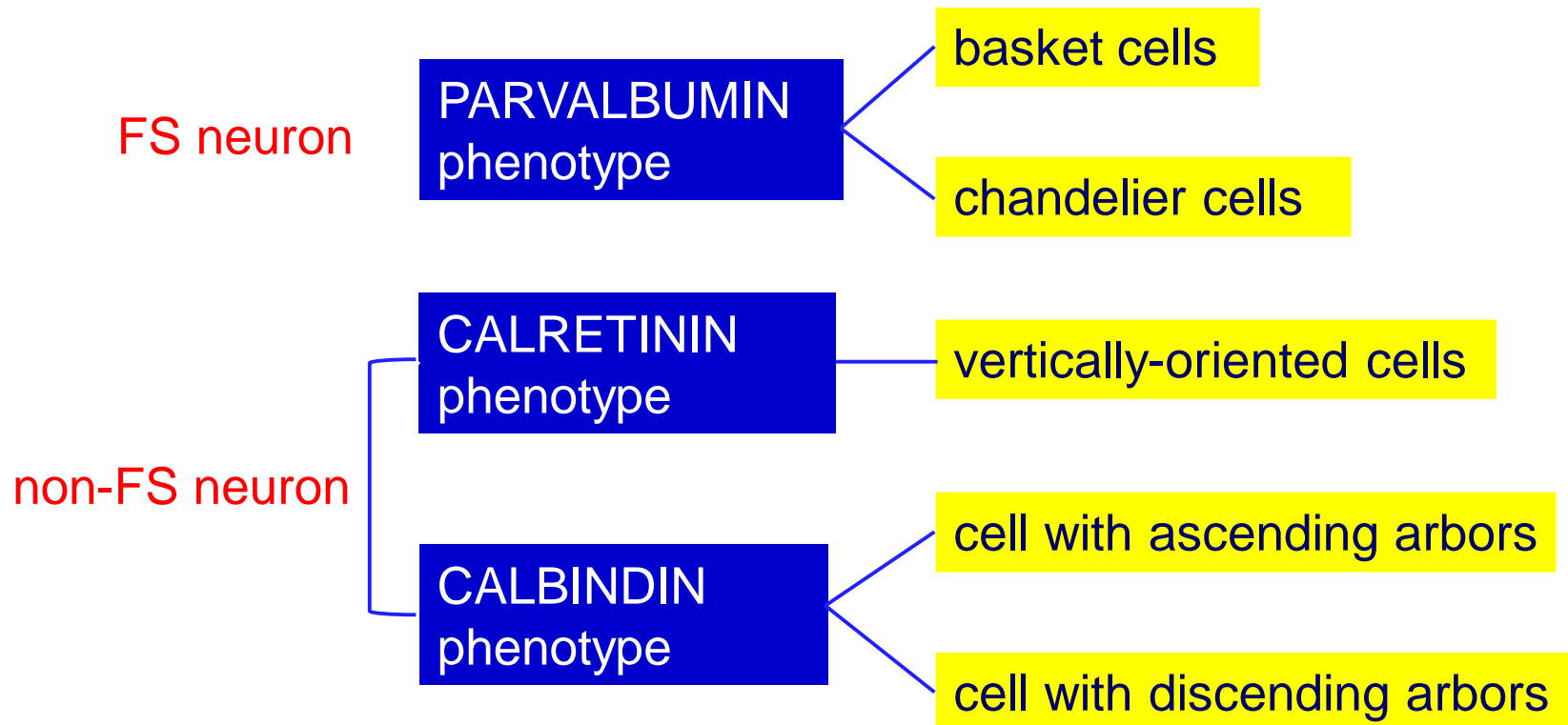


Figure 4. Hierarchical tree plot illustrating the results of cluster analysis. There are two main branches corresponding to FS interneurons (FSI) and non-FS cells. The first cluster mainly contained PV-positive interneurons and the second one consisted exclusively of CB- and CR-positive cells.

CONCLUSIONS:

- parvalbumin-expressing interneurons are exclusively FS
- calretinin- and calbindin-expressing interneurons are mainly non-FS
- multiple morphologies can correspond to a single functionally-defined phenotype



Electrophysiological and gene expression profiling of neuronal cell types

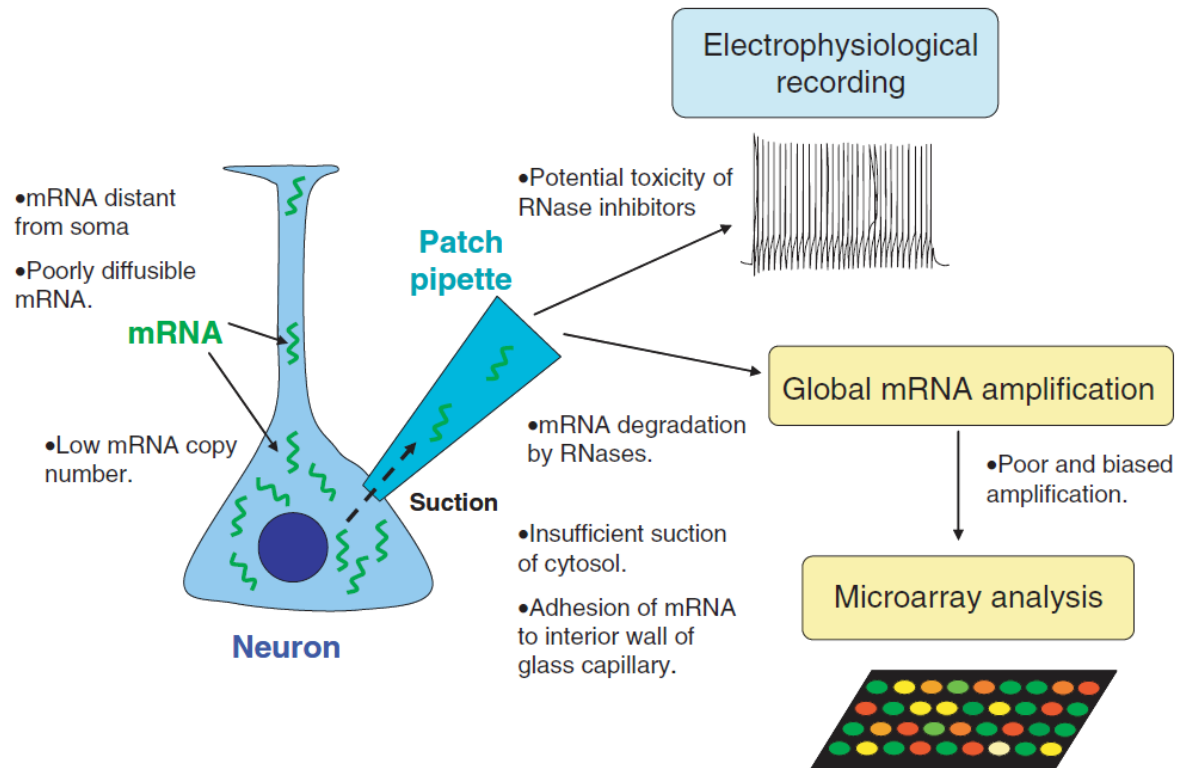


Figure 1. Potential problems with single-cell gene expression profiling by cytoplasmic harvesting via patch-pipette

Collecting extremely low amounts of mRNA from single cells is the biggest challenge of this technique. Only a small proportion of cytosol can be obtained by suction via patch-pipette, and poorly diffusible mRNA or dendritic mRNA are particularly hard to collect. The yield of mRNA can be improved by including inhibitors of RNases in the pipette, but these are often cytotoxic and can be detrimental to electrophysiological recording. It is also possible that some mRNA adheres to the interior wall of the glass capillary and evades expulsion from the patch-pipette.

another way to classify cortical interneurons is....

....to consider their **developmental origin:**

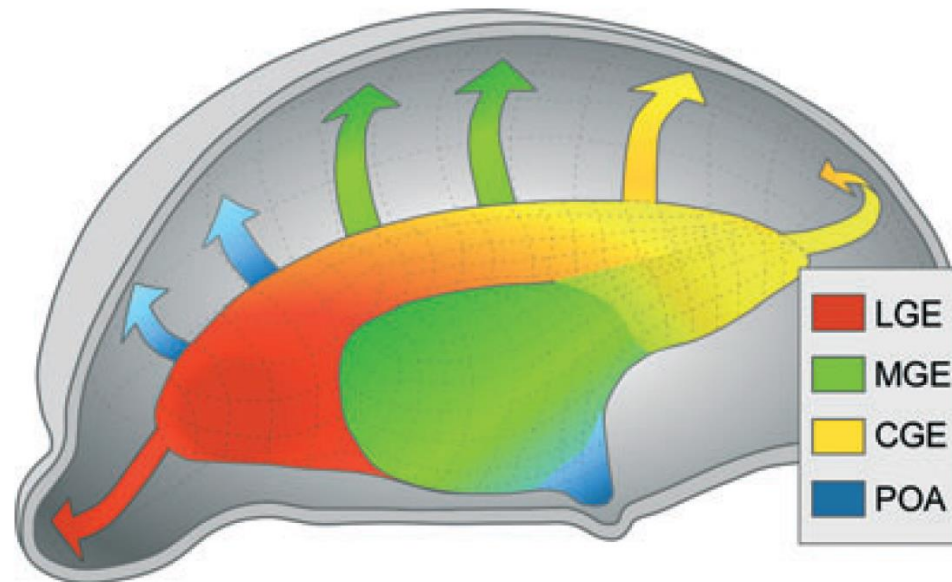


FIG. 2. Cortical interneurons are born in the subpallium and migrate tangentially to the cortex. The schema represents an E13.5 embryo brain hemisection. The arrows show representative migratory routes.

Cortical development

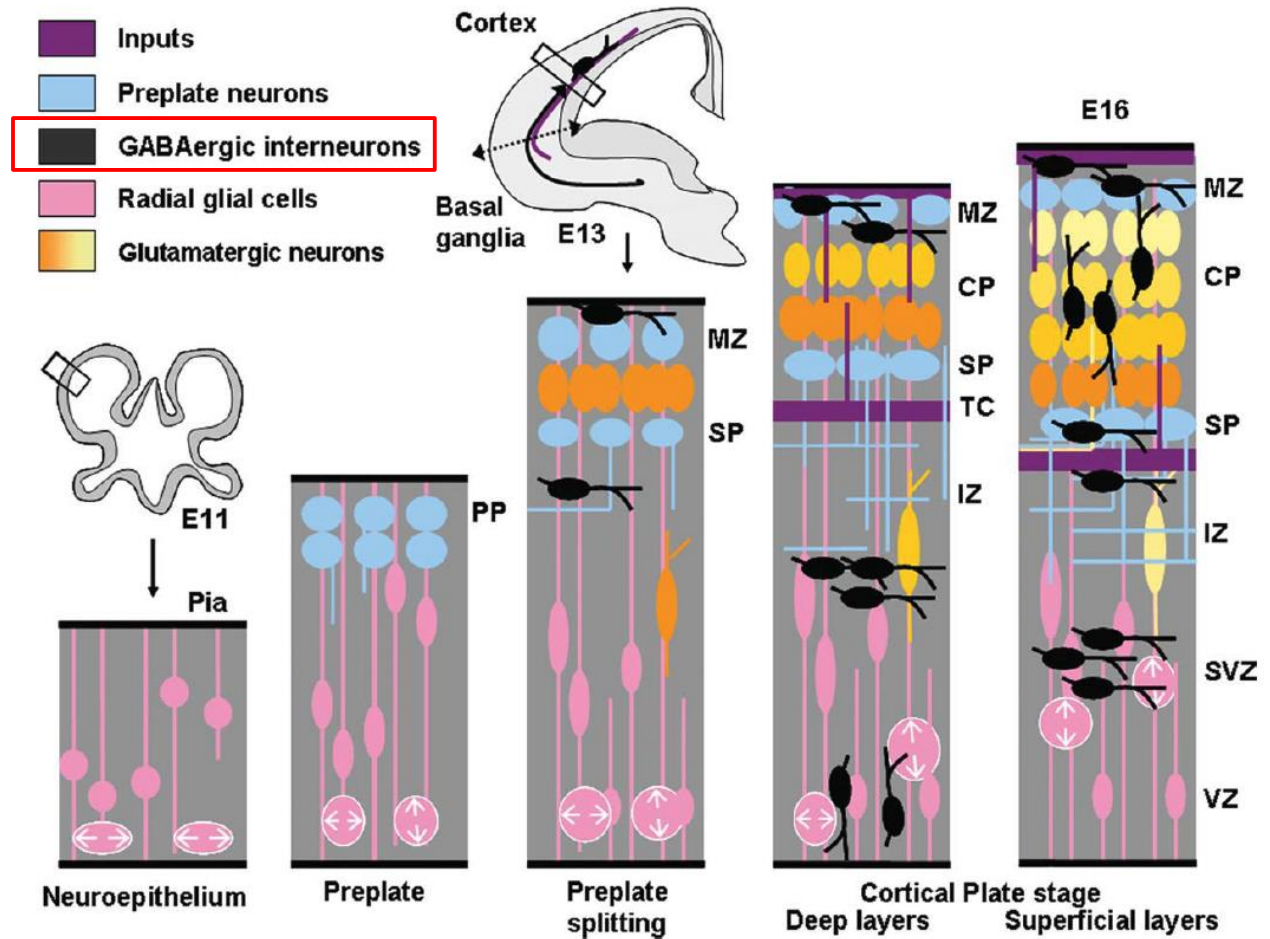
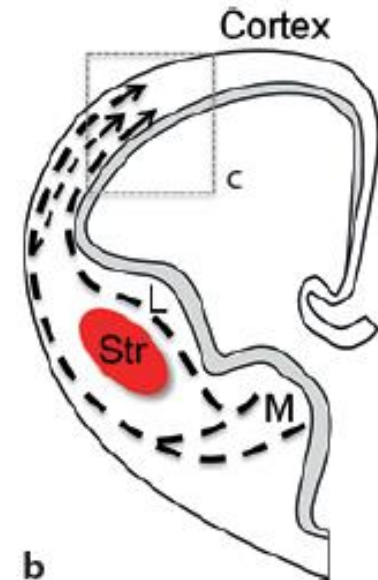
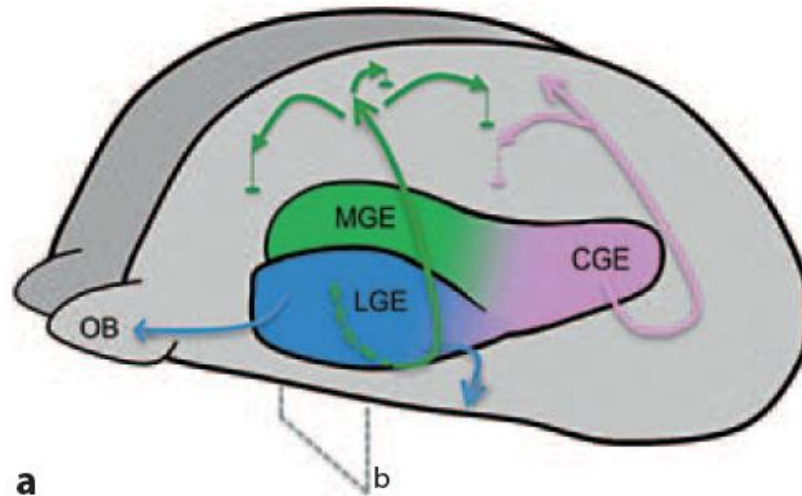


Figure 1 Cortical development. Schematic drawings of coronal sections of the developing mouse cortex. Afferent axons and the migration of telencephalic interneurons from the basal telencephalon are drawn in purple and black respectively. Cortical development begins with the appearance of a population of cells along the lateral ventricle, known as the ventricular zone (E11; VZ). This population of cells gives rise to most of the neurons and glial cells of the cerebral cortex. Once generated, neurons migrate towards the pial surface and complete their differentiation in the cortical plate. Neurons that will populate the deeper layers of the cortex are generated and then migrate away from the VZ earlier than the neurons that will populate progressively more superficial layers. On E12-E13, the cerebral wall is bilaminar consisting of the VZ and overlying primitive preplate. By E17-E18 the thickness of the overlying intermediate zone/with matter and developing cortical plate are at their maximum widths, with all neuronal cells having exited the cell cycle and migrated to their final laminar distribution within the developing cortex. CP, cortical plate; IZ, intermediate zone; MZ, marginal zone; PP, preplate; SP, subplate; TC, thalamocortical axons; SVZ, subventricular zone.

Primary routes of interneuron migration during cortical development.

Faux et al, 2012



Cortical interneurons born in the MGE and CGE in the ventral telencephalon follow tangential migratory paths into the developing cortex. Once within the cortical wall, cells disperse before entering the cortical plate and reside in a final position. The LGE-derived neurons migrate rostrally and ventrally into the olfactory bulb (OB) and striatum, respectively

Coronal section (indicated in a) illustrating the major routes of tangential migration through the embryonic telencephalon. Interneurons migrate from the MGE (M) and traverse the LGE (L) whilst avoiding the striatum (Str).

The Temporal and Spatial Origins of Cortical Interneurons Predict Their Physiological Subtype

Simon J.B. Butt,^{1,3} Marc Fuccillo,^{1,3} Susana Nery,^{1,4}
Steven Noctor,^{2,5} Arnold Kriegstein,^{2,5}
Joshua G. Corbin,^{1,6} and Gord Fishell^{1,*}

MGE-originating
interneurons

FS,
parvalbumin(somato
statin)-positive cells

CGE-originating
interneurons

non-FS,
calretinin(VIP, NPY)-
positive cells

Summary

Interneurons of the cerebral cortex represent a heterogeneous population of cells with important roles in network function. At present, little is known about how these neurons are specified in the developing telencephalon. To explore whether this diversity is established in the early progenitor populations, we conducted in utero fate-mapping of the mouse medial and caudal ganglionic eminences (MGE and CGE, respectively), from which most cortical interneurons arise. Mature interneuron subtypes were assessed by electrophysiological and immunological analysis, as well as by morphological reconstruction. At E13.5, the MGE gives rise to fast-spiking (FS) interneurons, whereas the CGE generates predominantly regular-spiking interneurons (RSNP). Later at E15.5, the CGE produces RSNP classes distinct from those generated from the E13.5 CGE. Thus, we provide evidence that the spatial and temporal origin of interneuron precursors in the developing telencephalic eminences predicts the intrinsic physiological properties of mature interneurons.

In utero fate-mapping of cortical interneurons ...

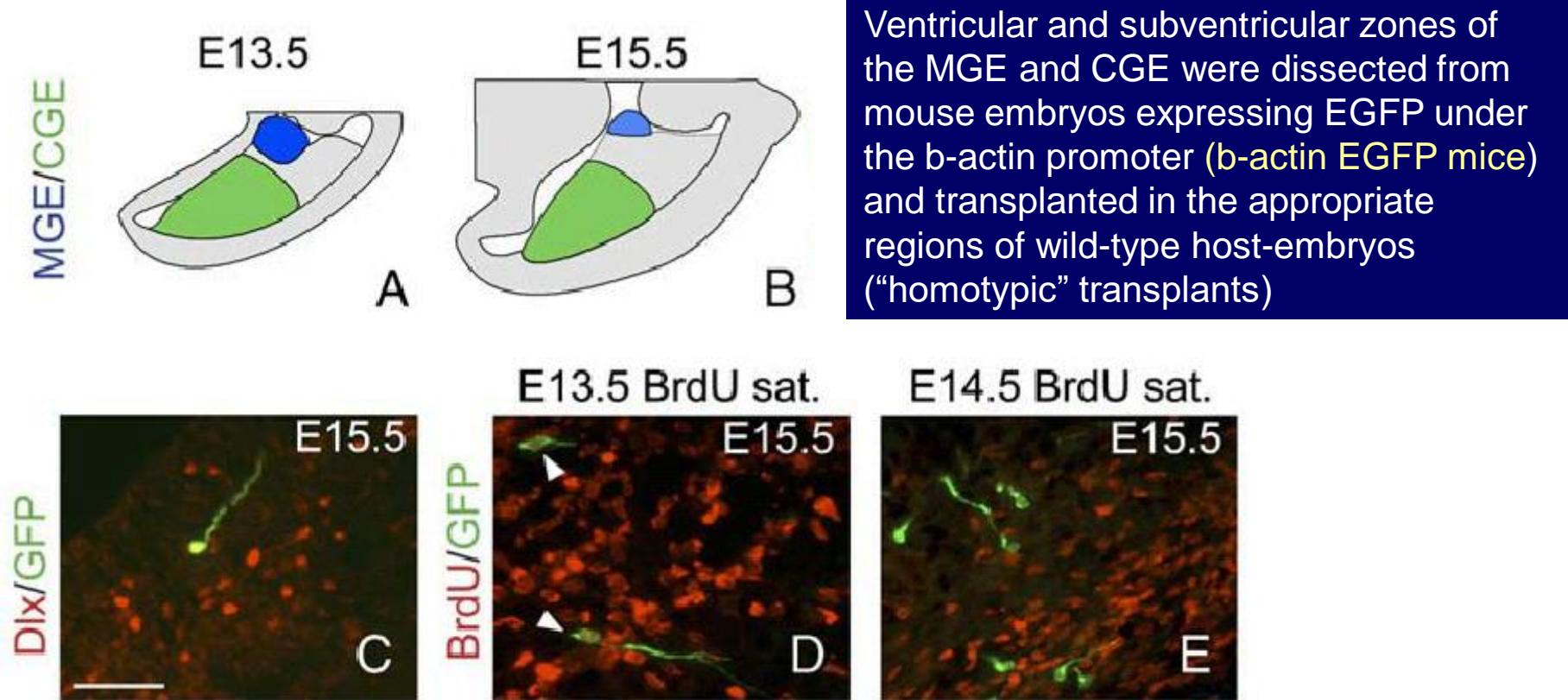
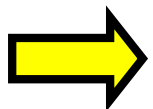


Figure 1. In Utero Fate-Mapping of the Ventral Telencephalic Eminences

(A and B) Schematic of the regions taken from the ventral telencephalon for in utero transplantation, as seen with the cortex removed and viewed from above. (C) Many transplanted progenitors expressed Dlx proteins, a characteristic of developing interneurons. BrdU saturation was performed immediately after transplantation (D) and 1 day following transplantation of MGE progenitors at E13.5 (E). Embryos sacrificed at E15.5 and stained with BrdU and GFP showed that while many progenitors proliferated immediately after transplantation (white arrowheads), after 1 day there were fewer proliferative transplanted neurons (E).



electrophysiological, immunocytochemical and morphological reconstruction of mature interneurons in young-adult mice

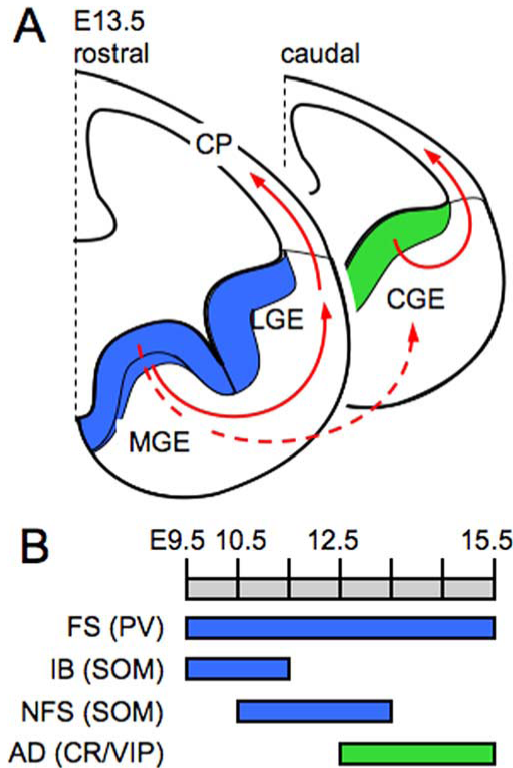


Figure 1. Subcortical origins of cortical interneurons in the mouse telencephalon. *A*, Diagram showing rostral and caudal coronal sections through an embryonic [embryonic day 13.5 (E13.5)] mouse telencephalon. The large majority of cortical interneurons originate from the proliferative zone (PZ) (the ventricular and subventricular zones) of two subcortical structures, the MGE (blue PZ) and CGE (green PZ), before migrating tangentially (filled red arrows) into the developing cortical plate (CP). Transplantation experiments suggest that interneurons from the MGE also migrate caudally (dashed red arrow) via the CGE before undergoing tangential migration. *B*, Evidence from both transplantation and genetic fate-mapping experiments has revealed distinct spatial and temporal origins for distinct physiological subtypes of interneuron as assayed by their intrinsic properties. The bulk of interneuron neurogenesis occurs from E9.5 until E15.5 (gray scale bar). Fast spiking interneurons, most of which express PV, burst spiking interneurons (IB), most of which express SOM, and SOM-positive nonfast spiking interneurons (NFS) originate from the MGE with different temporal profiles (blue histogram bars). Adapting (AD) interneurons, which primarily express CR and/or vasoactive intestinal peptide (VIP), originate at later time points from the CGE (green bar).

CONCLUSIONS:

- parvalbumin-expressing/FS/basket-shaped neurons originate from MGE
- calretinin-expressing/non-FS/bipolar (vertically-oriented?) neurons originate from CGE

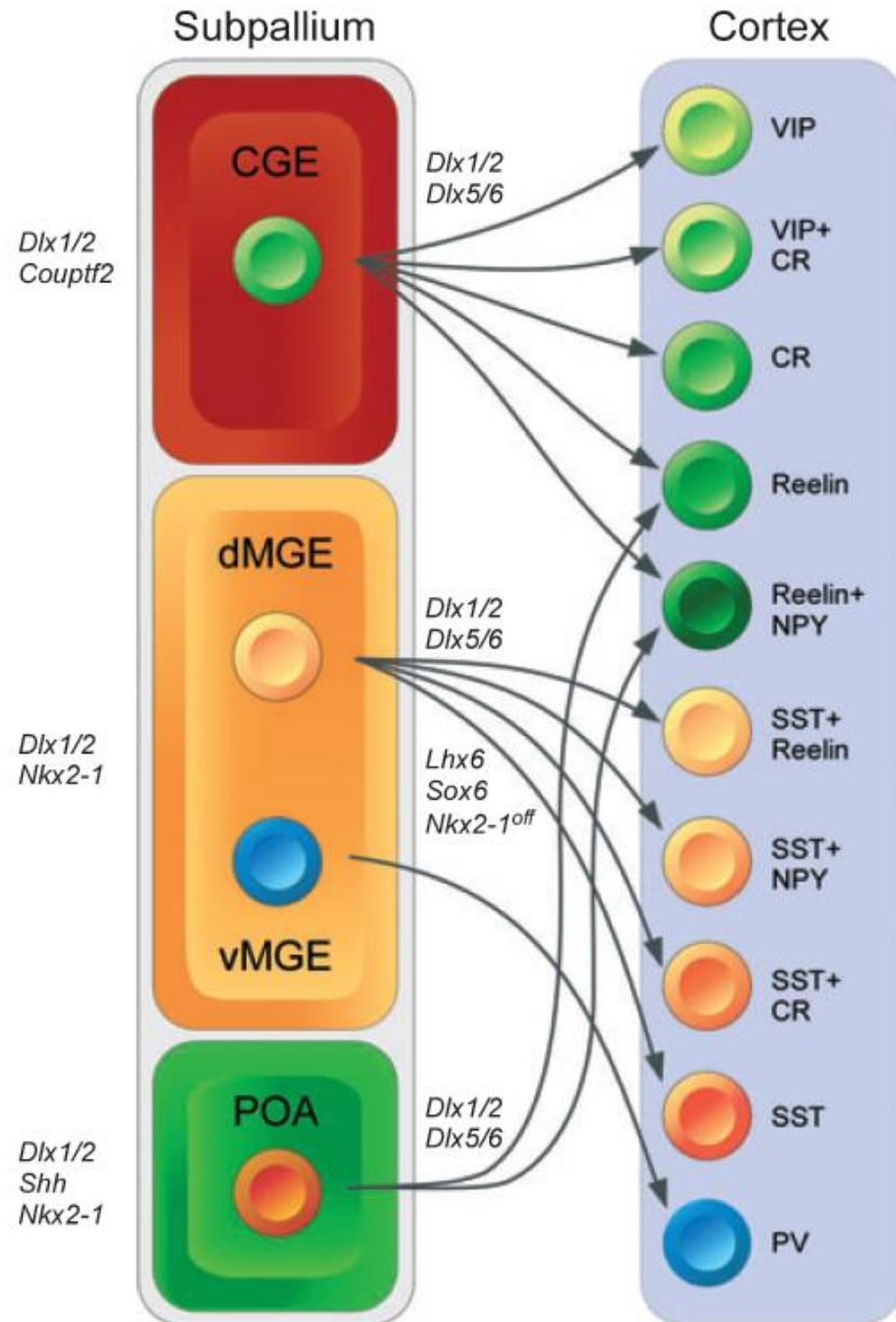
This means that different subtypes of interneurons are generated at different spatial positions (= from different progenitors)

CLASSIFYING neurons **BY THEIR ORIGIN** could be a new method of neuronal classification

Cortical interneuron diversity largely emerges from spatially segregated progenitor cells with distinct transcriptional profiles

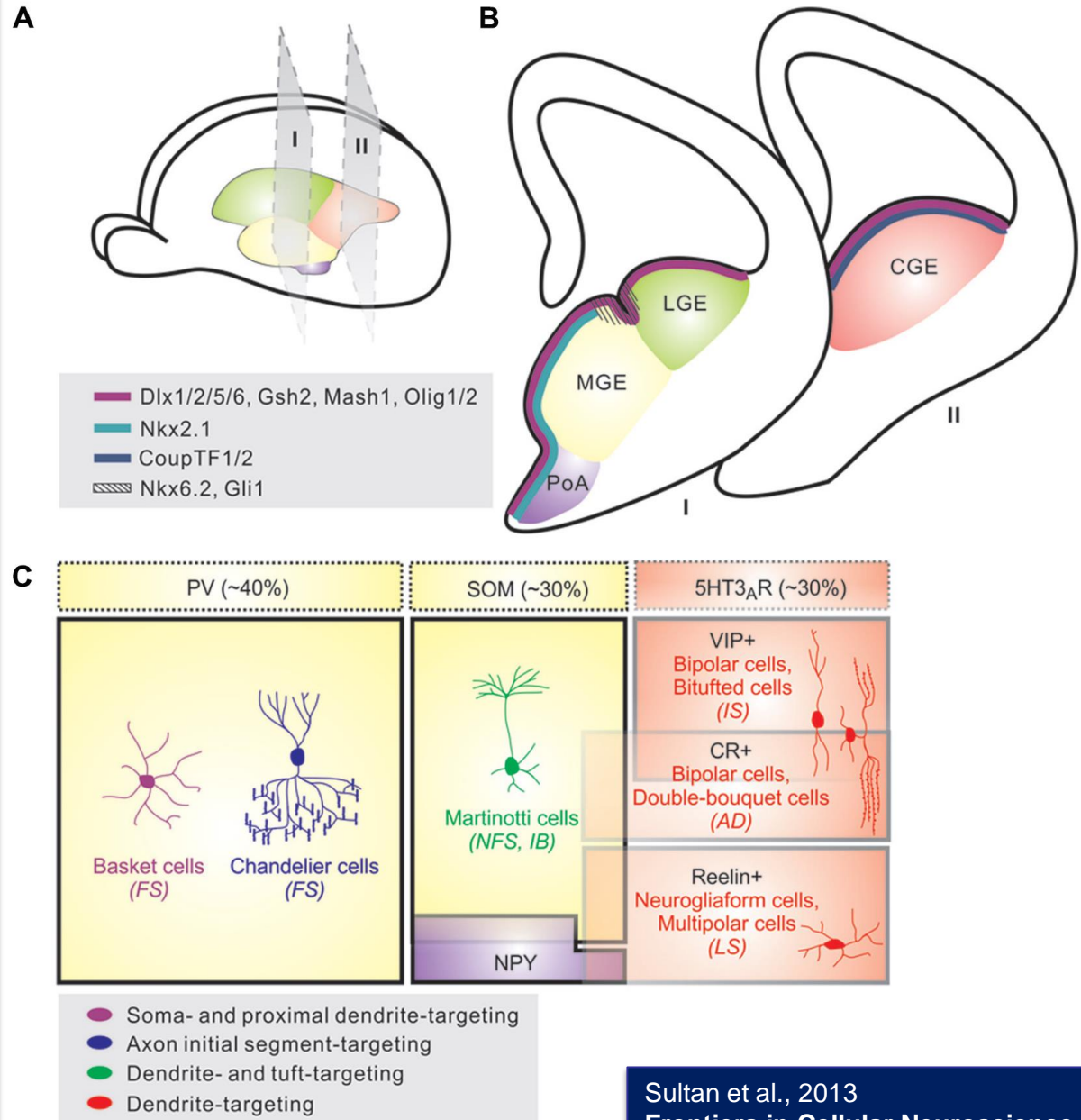
Gelman & Marin, 2010

FIG. 3. Cortical interneuron diversity largely emerges from spatially segregated progenitor cells with distinct transcriptional profiles. The schema shows the main sources of cortical interneurons, CGE, MGE and POA, which contain progenitor cells that can be distinguished by their expression of transcription factors and other proteins. Thus, CGE cells express both *Dlx1/2* and *Couptf2*, MGE cells express *Dlx1/2* and *Nkx2-1*, and POA cells express *Dlx1/2*, *Nkx2-1* and *Shh*. Furthermore, each of these regions seems to contain distinct progenitor domains (not shown in the schema), characterized by the expression of different transcription factors (Flames *et al.*, 2007). Each progenitor region produces a particular group of interneurons, although some interneuron classes may emerge from different progenitor domains. This is the case for multipolar reelin/NPY-containing interneurons, which derive from both CGE and POA. It is possible, however, that these cells derive from a progenitor domain that bridges the two structures and that is characterized by the expression of *Couptf2* (Kanatani *et al.*, 2008). Only the mechanisms involved in the generation of MGE cells are beginning to be elucidated. Thus, down-regulation of *Nkx2-1* and expression of *Lhx6* and *Sox6* are necessary for the proper specification of MGE-derived interneurons.



IN SUMMARY: Origins and diversity of neocortical interneurons

(A) Neocortical interneurons are derived from progenitor cells located in the proliferative zones of the ventral telencephalon, specifically within the medial ganglionic eminence (MGE) and caudal ganglionic eminence (CGE). A small proportion is produced in the preoptic area (PoA). **(B)** Various transcription factors are expressed in distinct patterns throughout the subpallial germinal zones. **(C)** Neocortical interneurons are highly diverse and can be defined based on morphology, neurochemical expression, electrophysiological properties, and subcellular synaptic targeting specificity.





Using Fluorescence Activated Cell Sorting to Examine Cell-Type-Specific Gene Expression in Rat Brain Tissue

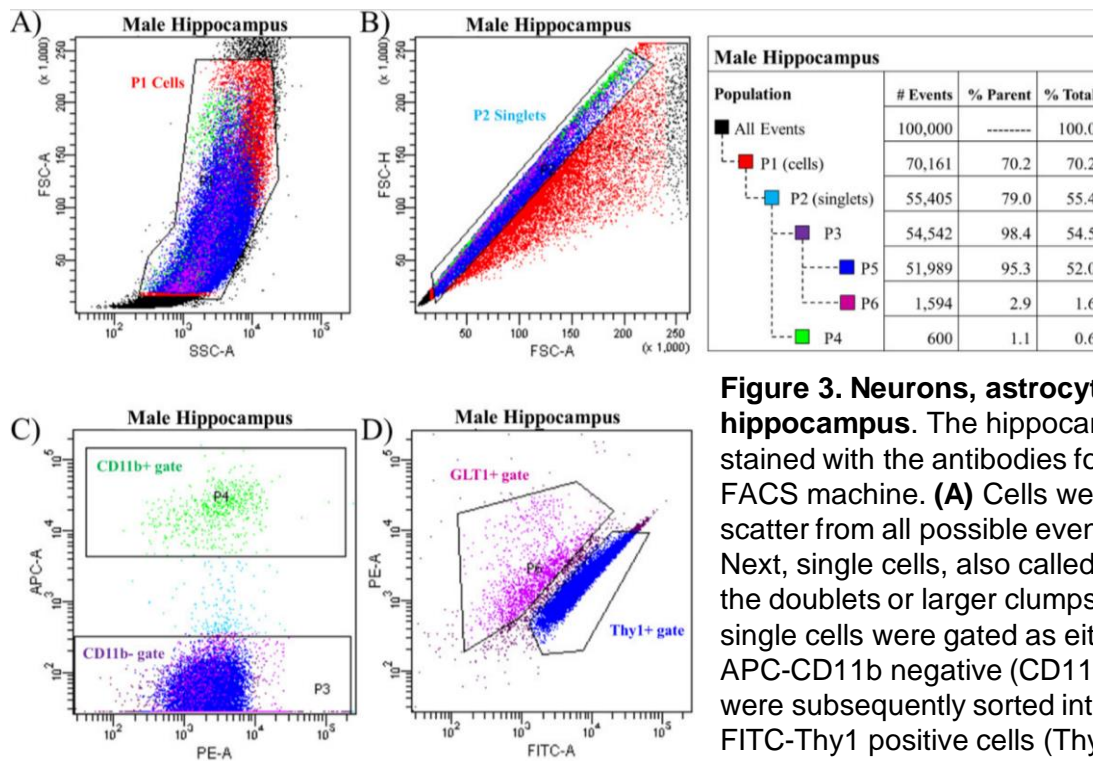


Figure 3. Neurons, astrocytes, and microglia sorted from a male hippocampus. The hippocampus from one male rat was dissociated and stained with the antibodies for CD11b, GLT1 and Thy1 and sorted using a FACS machine. **(A)** Cells were first sorted based on their forward and side scatter from all possible events. This gate is called P1 (population 1). **(B)** Next, single cells, also called singlets, were sorted based on their size from the doublets or larger clumps of cells. This gate is called P2. **(C)** Third, the single cells were gated as either APC-CD11b positive (CD11b+ gate, P4) or APC-CD11b negative (CD11b- gate, P3). **(D)** APC-CD11b negative cells were subsequently sorted into PE-GLT1 positive cells (GLT1+ gate, P6) and FITC-Thy1 positive cells (Thy1+ gate, P5). The breakdown of all events and all gates was generated from the FACS software depicted in a table which is presented on the right.

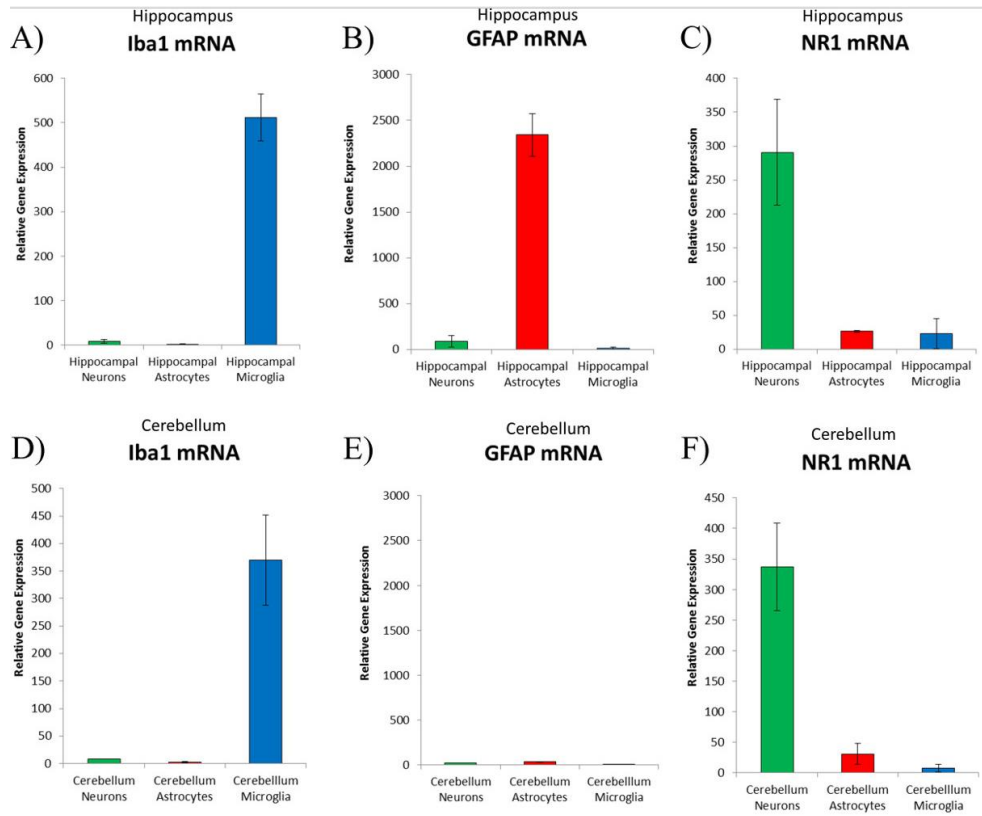


Figure 5. Real-time PCR analysis of cell-type-specific genes from sorted cells. Neurons (green bars), astrocytes (red bars) and microglia (blue bars) were sorted based on the protocol described above and mRNA was extracted for confirmation of cell-type-specific gene expression. **(A)** Iba1 is a calcium binding protein expressed exclusively in microglia sorted from the male hippocampus. **(B)** GFAP is a filament protein expressed predominantly in astrocytes sorted from the male hippocampus **(C)** NR1 is a ubiquitous subunit of the NMDA glutamatergic receptor that was expressed predominantly on neurons sorted from the male hippocampus. **(D)** Iba1 was also expressed exclusively on microglia sorted from the male cerebellum. **(E)** Interestingly, GFAP was not expressed in any of the cell types sorted from the male cerebellum. **(F)** The NR1 subunit of the NMDA receptor was also expressed predominantly on neurons sorted from the male cerebellum.

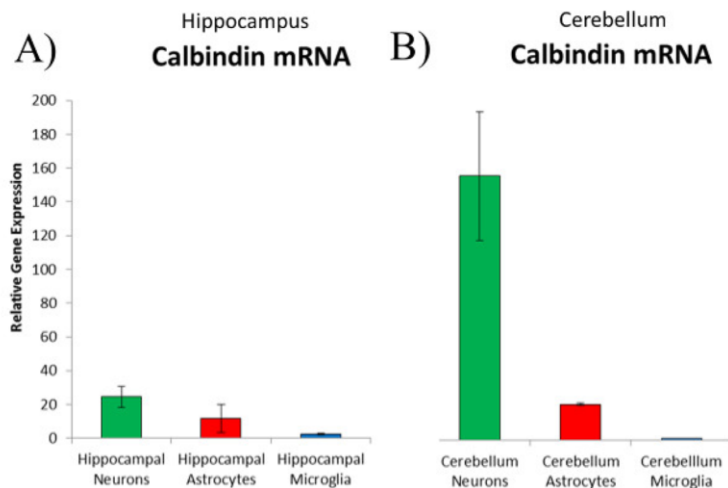


Figure 6. Real-time PCR analysis of calbindin expressed in sorted neural cells. Cells sorted using FACS can be used to analyze cell-typespecific gene expression. **(A)** Neurons (green bars) expressed significantly more Calbindin than either astrocytes (red bars) or microglia (blue bars) sorted from the male hippocampus. **(B)** Neurons sorted from the male cerebellum expressed significantly higher levels of Calbindin than either astrocytes or microglia sorted from the cerebellum, but also significantly higher levels than the neurons sorted from the hippocampus.

Cell types in the mouse cortex and hippocampus revealed by single-cell RNA-seq*

Zeisel et al., 2015 Science 347:1138-1142

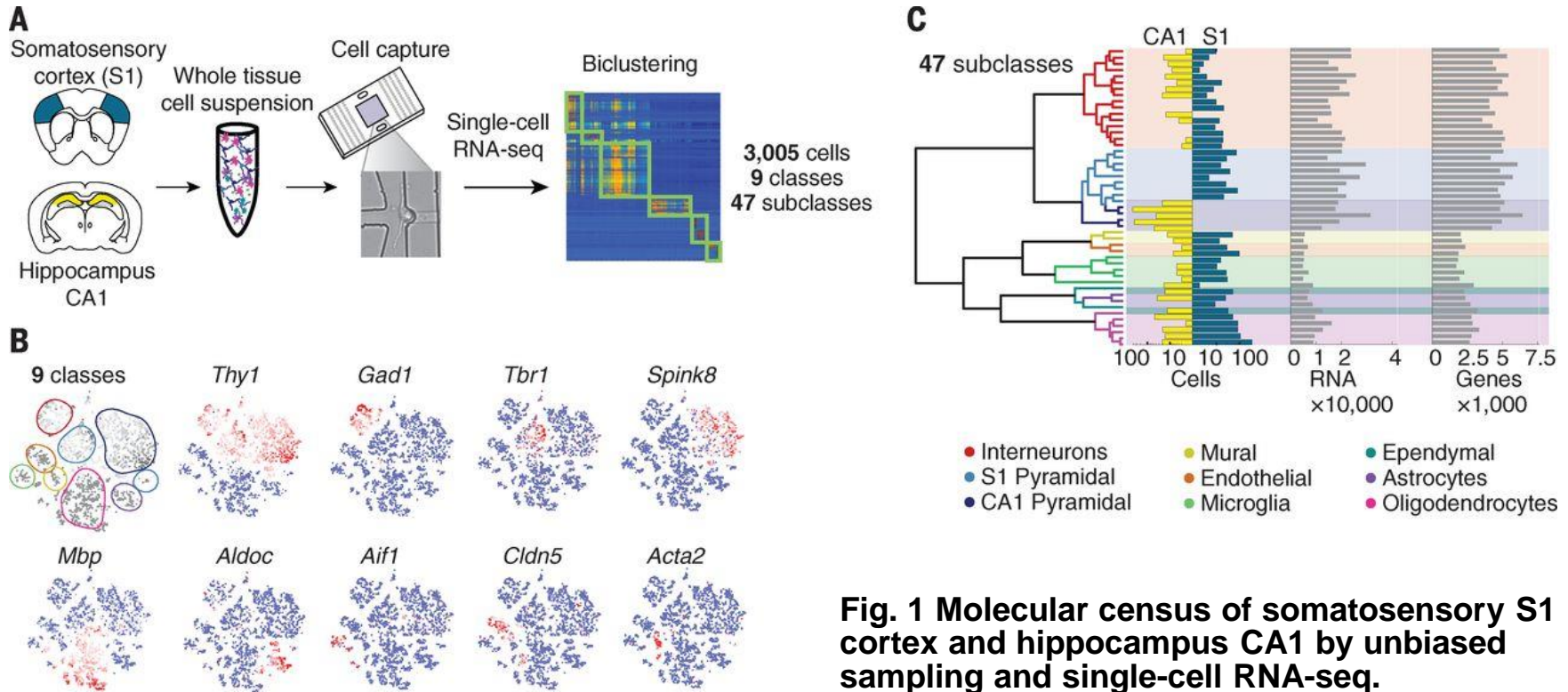
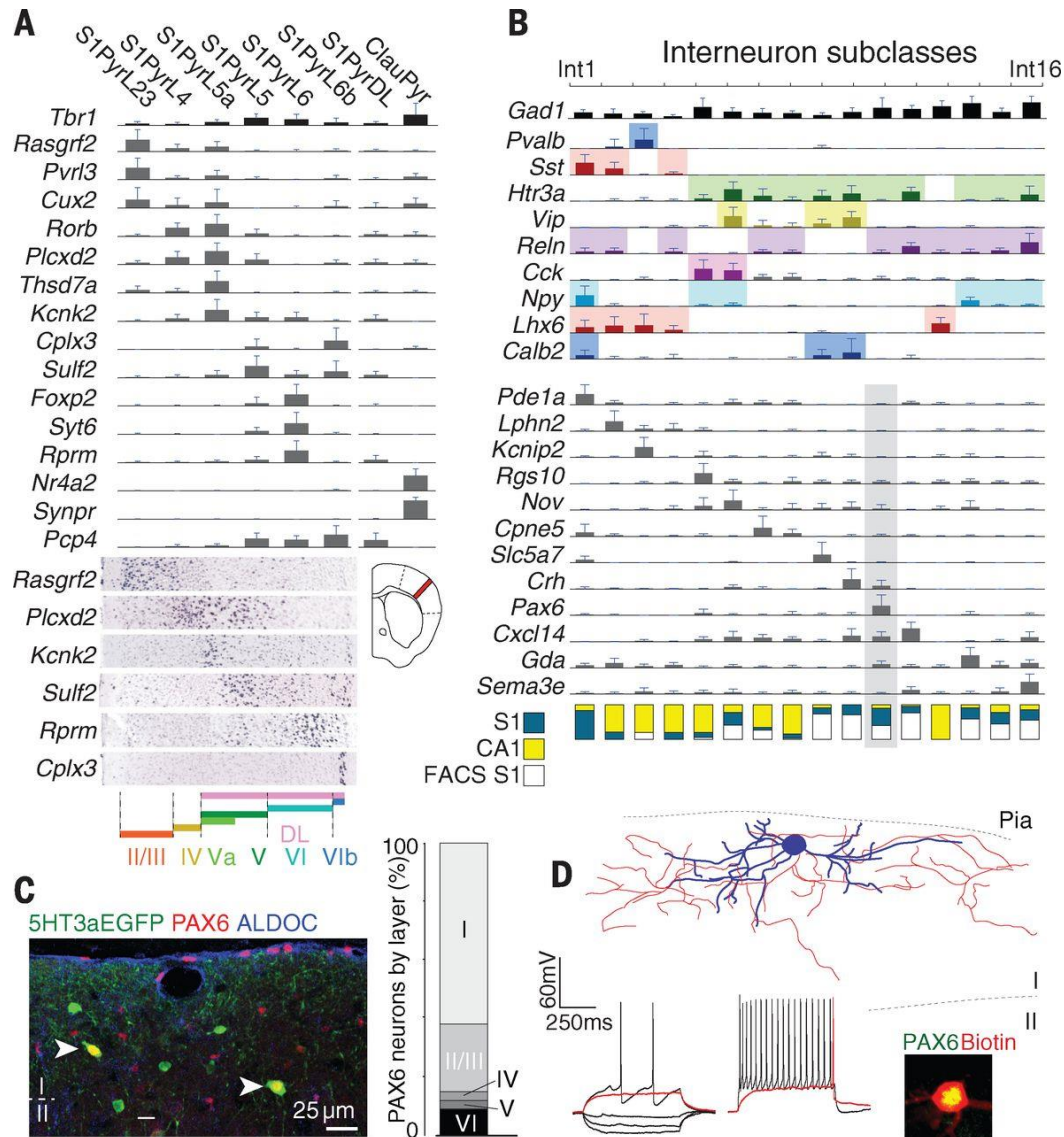


Fig. 1 Molecular census of somatosensory S1 cortex and hippocampus CA1 by unbiased sampling and single-cell RNA-seq.

(A) Workflow for obtaining and analyzing single-cell RNA-seq from juvenile mouse cortical cells, from dissection to single-cell RNA-seq and biclustering. **(B)** Visualization of nine major classes of cells using t-distributed stochastic neighbor embedding (tSNE). Each dot is a single cell, and cells are laid out to show similarities. Colored contours correspond to the nine clusters in (A) and fig. S3. Expression of known markers is shown using the same layout (blue, no expression; white, 1% quantile; red, 99% quantile). **(C)** Hierarchical clustering analysis on 47 subclasses. Bar plots show number of captured cells in CA1 and S1, number of detected polyA+ RNA molecules per cell, and total number of genes detected per cell.

* **RNA-Seq (RNA sequencing)**, uses **next-generation sequencing (NGS)** to reveal and quantify the whole transcriptome in a biological sample. See Mutz et al., 2013 (Current Opinion in Biotechnology, 24:22–30) for review of the technique

Fig. 2 Neuron subclasses in the somatosensory cortex



(A) Subclasses of pyramidal neurons in the somatosensory cortex (S1) identified by BackSPIN clustering. Bar plots show mean expression of selected known and novel markers (error bars show standard deviations). Layer-specific expression shown by in situ hybridization (Allen Brain Atlas). S1PyrL23, layer II-III; S1PyrL4, layer IV; S1PyrL5a, layer Va; S1PyrL5, layer V; S1PyrL6, layer VI; S1PyrL6b, layer VIb; S1PyrDL, deep layers; ClauPyr, claustrum.

(B) Identification of interneuron subclasses. Bar plots show selected known and novel markers. Fraction of S1/CA1 cells is depicted at bottom: blue, S1; yellow, CA1; white, flow-sorted Htr3a+ cells from S1.

(C) Immunohistochemistry demonstrating the existence and localization of novel PAX6+/5HT3aEGFP+ interneurons, Int11. Bar plots show the layer distribution of these neurons. **(D)** Intrinsic electrophysiology and morphology of PAX6+ interneurons in S1 layer I, identified by post hoc staining.

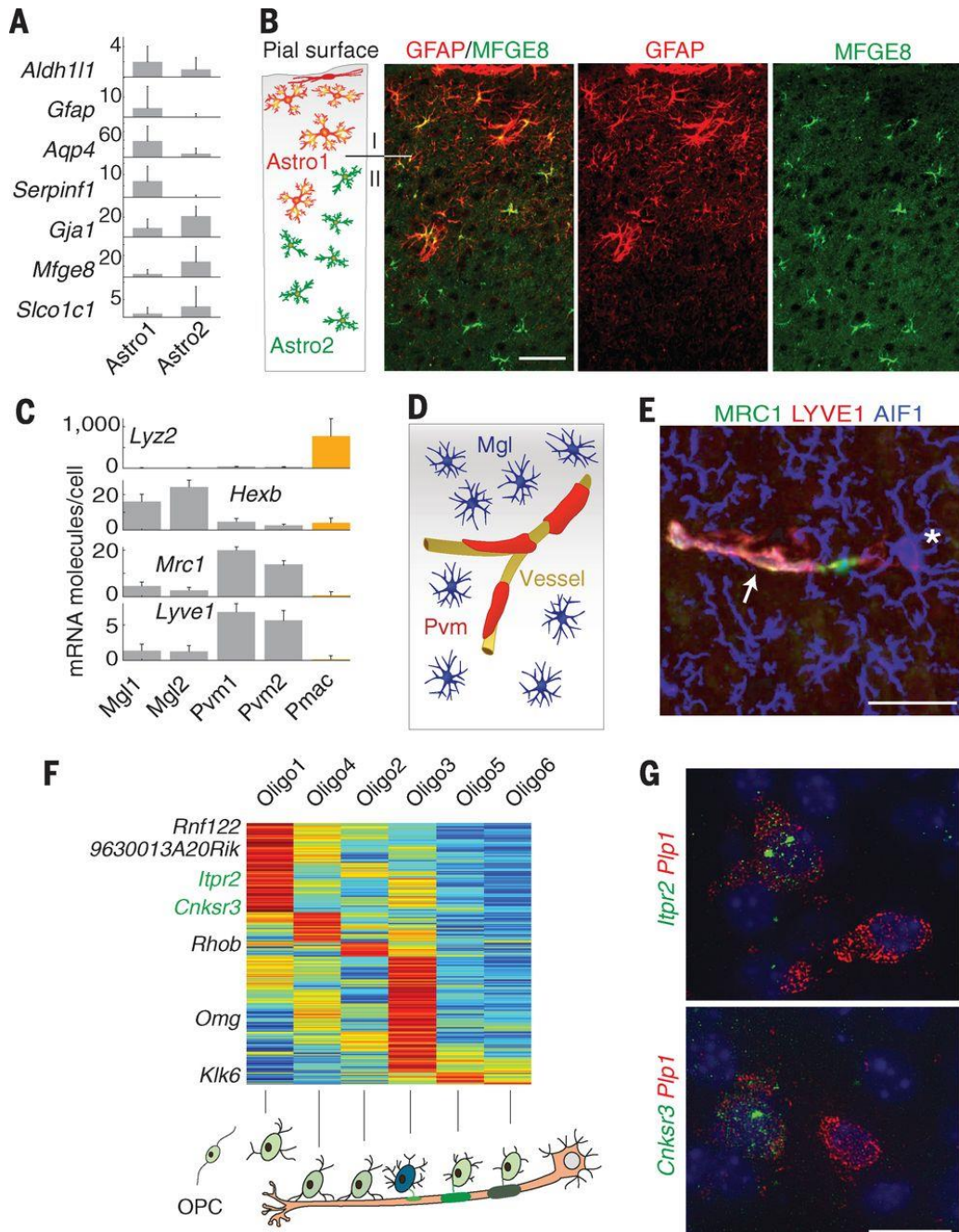


Fig. 3 Characterization of glial subclasses.

(A) Two types of astrocytes (Astro1 and Astro2) identified by common and distinct markers.

(B) Immunohistochemistry for glial fibrillary acidic protein (red, Astro1) and MFGE8 (green, Astro2). Scale bar, 50 mm.

(C) Genes showing expression restricted to microglia (Mgl), perivascular macrophages (Pvm), and peritoneal macrophages (Pmac). Error bars show standard deviations.

(D) Cartoon illustrating the morphology and localization of microglia and perivascular macrophages.

(E) Immunostaining for AIF1 (previously known as Iba-1, blue) marking microglia, and for MRC1 (green) and LYVE1 (red) marking perivascular macrophages. Asterisk, a microglia cell. Arrow, a perivascular macrophage aligned to a vessel (not stained). Scale bar, 20 mm.

(F) Heat map showing progressive changes in gene expression along oligodendrocyte differentiation, illustrated below.

(G) Single-molecule RNA FISH for *Itpr2* and *Cnksr3* mark a strict subset of oligodendrocytes (as identified by *Plp1*). Scale bar, 11 mm.